

Kit Ligand and Kit receptor tyrosine kinase sustain synaptic inhibition of Purkinje Cells

Reviewed Preprint

Revised by authors after peer review.

[About eLife's process](#)

Reviewed preprint version 2

January 24, 2024 (this version)

Reviewed preprint version 1


August 14, 2023

Sent for peer review

June 7, 2023

Posted to preprint server

May 30, 2023

Tariq Zaman, Daniel Vogt, Jeremy Prokop, Qusai Abdulkhaliq Alsabia, Gabriel Simms, April Stafford, Bryan W. Luikart, Michael R. Williams 

Department of Pediatrics & Human Development, College of Human Medicine, Michigan State University • Office of Research, Corewell Health • Department of Molecular and Systems Biology, Geisel School of Medicine at Dartmouth College

 https://en.wikipedia.org/wiki/Open_access

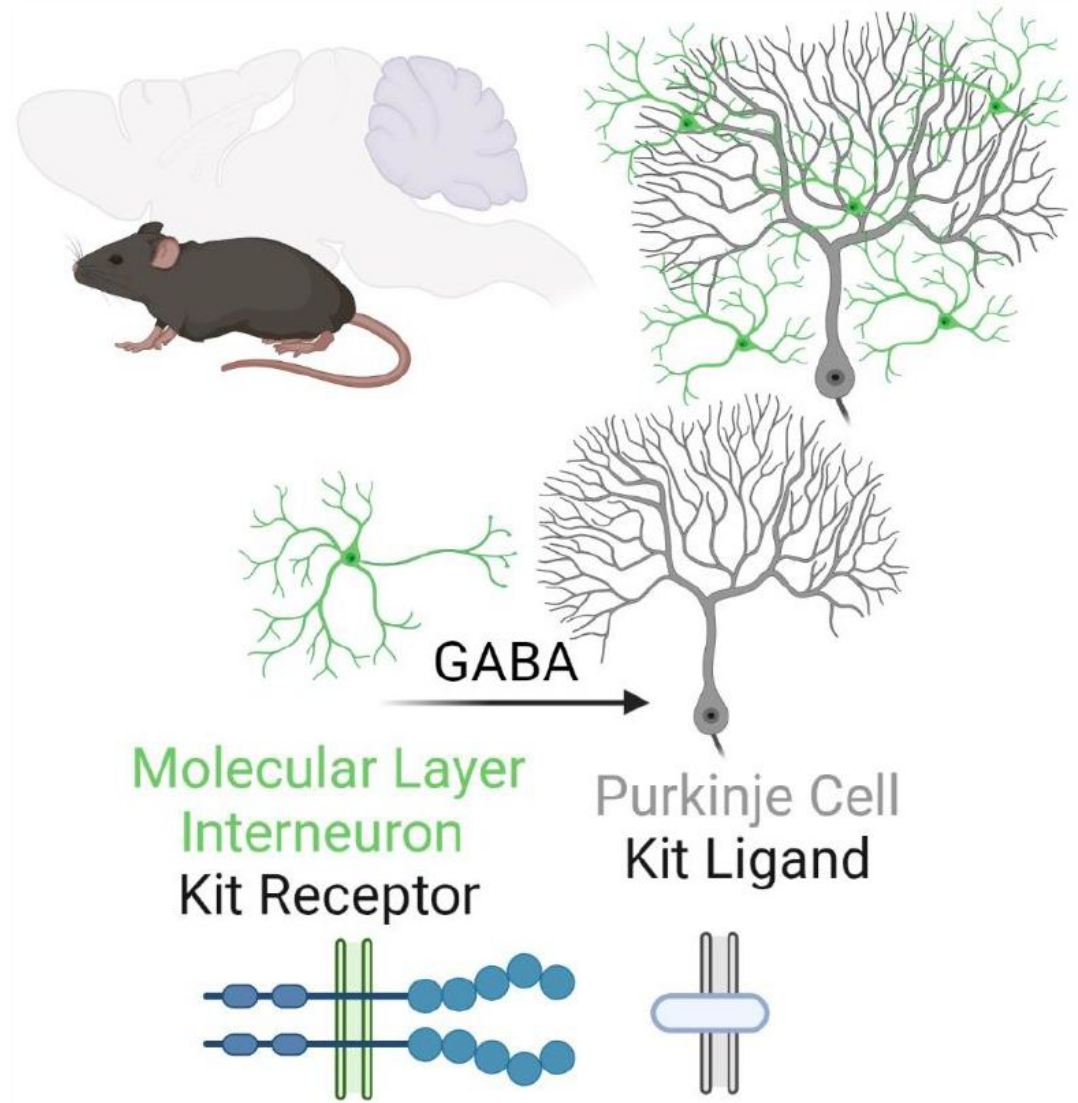
 Copyright information

Abstract

Summary

The cell-type specific expression of ligand/receptor and cell-adhesion molecules is a fundamental mechanism through which neurons regulate connectivity. Here we determine a functional relevance of the long-established mutually exclusive expression of the receptor tyrosine kinase Kit and the trans-membrane protein Kit Ligand by discrete populations of neurons in the mammalian brain. Kit is enriched in molecular layer interneurons (MLIs) of the cerebellar cortex (i.e., stellate and basket cells), while cerebellar Kit Ligand is selectively expressed by a target of their inhibition, Purkinje cells (PCs). By *in vivo* genetic manipulation spanning embryonic development through adulthood, we demonstrate that PC Kit Ligand and MLI Kit are required for, and capable of driving changes in, inhibition of PCs. Collectively, these works in mice demonstrate that the Kit Ligand/Kit receptor dyad sustains mammalian central synapse function and suggest a rationale for the affiliation of Kit mutation with neurodevelopmental disorders.

Visual Abstract



eLife assessment

This **valuable** study from Zaman et al. demonstrates that the cKit-Kit ligand complex is necessary for the formation and/or maintenance of molecular layer interneuron synapses in cerebellar Purkinje cells. The evidence presented is **convincing**; in particular, the use of cell-type specific knockout of cKit in molecular layer interneurons and knockout of Kit ligand in Purkinje cells provides robust evidence. This work will be of particular relevance to those interested in inhibitory synapse formation or the role of inhibition in Purkinje cell behavior.

Introduction

The proto-oncogene receptor tyrosine kinase Kit (c-Kit, CD117) is an evolutionarily conserved, loss-of-function intolerant, gene that is enriched in specific neuron populations and tentatively associated with rare cases of neurological dysfunction (pLI= 0.98 and LOEUF of 0.17) (**Figure**

S1A,B [1, 2]. It is perhaps unsurprising that loss-of-function Kit mutations in humans are rare; Kit is highly pleiotropic, supporting diverse cell populations including melanocytes, hematopoietic stem/progenitor cells, germ cells, mast cells, and interstitial cells of Cajal [3]. Thus, Kit mutations can result in diverse conditions such as hypo- or hyperpigmentation or melanoma, anemia or leukemia, infertility, mastocytosis, and impaired gut motility or gastrointestinal tumors (Kit biology reviewed [4]).

The activation of Kit is stimulated by Kit Ligand (Gene symbol KITLG, herein KL), a single-pass transmembrane protein having an extracellular active domain that induces Kit dimerization and kinase activity. Across several decades and species, it has been reported that KL and Kit are mutually expressed in discrete neuron populations known to be connected; it has thus been hypothesized that the expression pattern of KL-Kit may reflect a role in connectivity [5-8]. Consistent with such a function, case reports have implicated inactivating Kit mutations with disorders of the central nervous system (References [9-13] and **Figure S1C**). Clinical phenotypes include developmental delay, ataxia, hypotonia, intellectual disability, deafness, and autism spectrum disorder. White matter abnormalities have been noted, and limited evidence suggests KL-Kit may indeed regulate axon outgrowth. KL or Kit mutation or pharmacological manipulation alters outgrowth of spinal commissural axons *in vitro* [14], KL stimulates cortical neurite outgrowth *in vitro* [15], and Kit reduction in cortex of developing rats or mice delays axon extension [16]. While these reports provide anatomical/morphological data suggesting that KL-Kit influences connectivity, these studies did not address consequences to neuronal physiology or synaptic connectivity. Functional studies of KL-Kit in synaptic physiology have likely been hampered by pleiotropy and organismal or cell death. Severe global KL-Kit hypomorphs exhibit fatal anemia, and developmental Kit depletion or inhibition in the cerebrum has resulted in the death of neuronal progenitors or nascent neurons [16-18]. Therefore, whether KL-Kit is necessary for synaptic function has remained largely unstudied. Here, we address this gap.

In mice, rats, and humans, Kit is abundantly expressed by molecular layer interneurons (MLIs) of the cerebellar cortex [6-8, 19], while cerebellar KL is restricted to Purkinje cells (PCs), which MLIs provide GABAergic synaptic inhibition to. We tested the hypothesis that PC KL and MLI Kit were essential to the GABAergic inhibition of PCs. We created a Kit conditional knockout mouse and accomplished embryonic knockout of Kit from MLIs; separately, we knocked out KL from postnatal PCs. By either method, disruption of the KL-Kit pair produced robust and specific impairments to GABAergic inhibition of PCs. Through sparse postnatal viral manipulation of KL in PCs, we provide evidence that KL functions throughout adulthood to regulate synaptic function. These results demonstrate that cell-type specific expression of KL and Kit influences functional connectivity in the mammalian brain, informing the long-observed expression of KL-Kit in the brain and suggesting a rationale for the affiliation of Kit loss with neurological impairment.

Methods

Animals

All procedures performed at Michigan State University were approved by the Institutional Animal Care and Use Committees of Michigan State University, which is accredited by the Association for Assessment and Accreditation of Laboratory Animal Care (AAALAC). Mice were on a 12-hour dark/light cycle, with *ad libitum* food and water. Male and female mice were used for all experiments. Mice were genotyped in-house using standard PCR-based methods, or via Transnetyx.

Creation of Kit conditional knockout mouse

We generated a strain of mice having exon 4 of Kit flanked by LoxP sites (“floxed”). This was accomplished by utilizing the services of UNC Animal Models Core (Dr. Dale Cowley) to generate chimeras from an ES cell line having a Knockout-first Allele (with conditional potential) for Kit (HEPD0509_8). The ES clones were obtained through the EuMMCR (European Mouse Mutant Cell Repository) of the EUCOMM (European Conditional Mouse Mutagenesis Program) [20]. Chimeric mice were screened for germline transmission of the targeted allele and were then crossed to a Flp deleter strain (C57BL/6N-Albino-Rosa26-FlpO) to convert the knockout-first allele to a conditional allele (tm1c) through removal of the FRT-flanked selection cassette. F1 male offspring carrying Kit tm1c and Flp alleles were crossed to C57Bl6/J females; we selected resultant progeny heterozygous for Kit tm1c but negative for Flp and the selection cassette. The Kit tm1c allele was bred to homozygosity while selecting against animals carrying the Tyr c-Brd allele (previously conveyed by C57BL/6N-Albino-Rosa26-FlpO). The resultant strain of mice having the Kit floxed tm1c allele are given the nomenclature C57BL/6N-Kit^{tm1c(EUCOMM)Mirow}/J; the Mirow lab code is registered through the National Academies to the author and principal investigator herein, **Michael Roland Williams**. Additional strains of mice used were Pax2-Cre transgenic mice (STOCK Tg(Pax2-cre)1Akg/Mmnc, RRID:MMRRC_010569-UNC [21]), Kit eGFP (Tg(Kit-EGFP)IF44Gsat/Mmucd; Gensat) [22] backcrossed for greater than 5 generations to C57Bl6/J (Stock No: 000664, The Jackson Laboratory), KitL floxed (Kitltm2.1Sjm/J, Stock #017861) [23], and Pcp2-Cre (Stock # 004146) mice [24], via The Jackson Laboratory.

To produce mixed litters of “Control” and “Kit KO” animals, mice homozygous for the Kit tm1c allele but negative for Pax2-Cre were crossed to mice homozygous for the floxed allele and Pax2-Cre positive. We used Kit KO females crossed to Control males as our breeding scheme. Experimental animals were derived from at least 5 generations of backcrossing Kit KO animals to Kit tm1c homozygous animals derived from a separate (Kit tm1c homozygous x Kit tm1c homozygous) breeding cohort.

Validation of Kit knockout

We investigated conditional knockout of Kit protein from the cerebellum by Western blot of total protein lysates from acutely harvested cerebellums (~P52) and by indirect immunofluorescence on free-floating vibratome-generated sections of transcatheter-perfused formaldehyde-fixed mouse brains (~P31). Western blots were probed with Rabbit: α -Kit (1:1000, clone D13A2, Cell Signaling Technologies product 3074), α -GAPDH (1:2000, Clone 14C10, product 2118 Cell Signaling Technology), or α -parvalbumin antibody (1:3000, product PV-27, Swant), each primary was detected via HRP conjugated Goat α -Rabbit secondary antibody (1:4000, Bio-Rad, product 170-6515) after incubation with Clarity ECL substrate (Bio-Rad, 1705061), via a Bio-Rad ChemiDoc MP.

For subsequent imaging and electrophysiology, we focused on lobule IV/V of the cerebellar cortex, as this area was superficially accessible for surgery, and provided a consistent area for focused comparisons between animals that would reduce the influence of spatial variations in KL or Kit expression.

For indirect immunofluorescence, primary antibodies were rat α -Kit (1:500, Rat α -Kit clone ACK4, ThermoFisher, product MA5-17836), mouse α -calbindin (1:2000, α -calbindin-D28K, CB-955, Sigma Aldrich), and rabbit α -parvalbumin (1:500, PV-27, Swant). Primaries were detected by Goat-host highly cross-adsorbed secondary antibodies coupled to Alexa 488, Cy3, or Alexa 647 (1:400, Jackson ImmunoResearch). Nuclei were labeled with DAPI, tissues were mounted in an anti-fade reagent, and fluorescent signals captured laser scanning confocal microscopy. Cell densities for MLIs (parvalbumin positive and/or calbindin negative somas of the molecular layer) were performed on Maximum Z-projections of 2.5 to 2.6 micron thick stacks, using the multi-point feature for counting somas, and the polygon ROI tool for determining the area of the Molecular Layer in which the somas were counted; results from two-technical replicates were averaged for each animal. The

polygon tool was also used for determining maximal PSD-95+ pinceau area. To determine the width of the molecular layer, seven linear ROIs per field of view of comparable locations of lobules IV/V were averaged to generate per animal layer thickness measurements. For analysis of synapses, we quantified puncta (of $0.05\text{-}5\ \mu\text{m}^2$ using the Analyze Particles function) in the molecular layer that were triple positive (each channel auto-threshold) for rabbit α -VGAT(1:500, 131 003), mouse α -Gephyrin (1:5000, 147 011), and Chicken α -Calbindin (1:500, 214 006), all from Synaptic Systems. For analysis of pinceau markers we utilized mouse α -Kv1.1 (1:250, K36/15), Kv1.2 (1:250, K14/16), and PSD-95 (1:200, K28/43), all from NeuroMab/AntibodiesInc.

Stereotaxic Procedures

Injections of replication-defective viral particles used protocols substantially similar to those previously published [25]. In brief, mice were brought to an anesthetic plane using inhaled isoflurane by a low-flow system (SomnoSuite, Kent); thermal regulation was assisted by heating pad, and pain managed through topical lidocaine and by intraperitoneal ketoprofen. A digital stereotaxic device (Kopf) and reference atlas were used to localize a small hole in the skull; cerebellar coordinates were: neonates; A/P, -2.55; M/L, - 1.1 (reference Lambda), D/V, 1.5 to 0.5 from dura; juvenile; A/P, -6.25; M/L, - 1.35; D/V, 1.5 to 0.75 (reference Bregma); adults; A/P, -6.35; M/L, - 1.8; D/V, 1.5 to 0.75 (reference Bregma). Viral particles were delivered via a ~30-gauge Hamilton Syringe controlled by digital syringe pump (WPI). The infused virus volume was 1-2 μl and there was a 5-minute period after infusion prior to needle withdrawal. Animals were monitored during and after operations. Ages for injection were, nominally, postnatal day (P) 7, 19, and 56; for P7 and P19, variability of up to two days was utilized to accommodate differences in animal size, and for P56 the eighth week of life was utilized.

Viruses

Lentiviral particles were derived from our vectors previously described to express transgenes under the hUbiC promoter and pseudotyped with VSV-G [26, 27]. Silent mutations disrupted the internal EcoRI sites of mouse KitL (MC204279, OriGene), the KitL coding sequence was then flanked by EcoRI sites, and the subsequent KitL coding sequence was introduced into a FUC-T2A-(EcoRI) plasmid, to create a FUC-T2A-KL-1 plasmid, wherein C designates mCherry. Subsequent deletion of KitL Exon 6 generated a KL-2 vector [28-31]. Sequences were verified by sequencing. Adeno-Associated Viral (AAV) particles were created by Vigene to drive Cre expression by the Purkinje Cell-Specific L7.6 promoter [32], or to drive mCherry or mCherry-T2A-KL-2 in a Cre-On fashion under the EF1 α promoter, with the AAV1 serotype.

Electrophysiology

For patch clamp electrophysiology of Control vs Kit KO, cells were recorded in slices generated from animals at 36.9 ± 0.6 and 37.4 ± 0.9 days for MLIs and PCs respectively. Analysis of the Pcp2 Cre mediated KL KO tissues was conducted similarly at ~40-44 days old. For viral PC KL KO animals injected as neonates (P7), juvenile (P19), and adults (P56) were recorded at an average of ~35, 45, and 83 days old, respectively. Avertin-anesthetized mice were perfused with a carbogen-equilibrated ice-cold slicing solution containing (in mM): 110 $\text{C}_5\text{H}_{14}\text{ClNO}$, 7 $\text{MgCl}_2 \cdot 6\text{H}_2\text{O}$, 2.5 KCl, 1.25 NaH_2PO_4 , 25 NaHCO_3 , 0.5 $\text{CaCl}_2 \cdot 2\text{H}_2\text{O}$, 10 Glucose, and 1.3 Na-Ascorbate. In the same solution, we generated 250-micron thick parasagittal sections of the cerebellum (Leica VT1200). Slices recovered at 34°C for 30 minutes in a carbogenated ACSF containing (in mM): 125 NaCl, 25 NaHCO_3 , 1.25 NaH_2PO_4 , 2.5 KCl, 1 $\text{MgCl}_2 \cdot 6\text{H}_2\text{O}$, 1 $\text{CaCl}_2 \cdot 2\text{H}_2\text{O}$ and 25 Glucose; slices were then held at room temperature for at least 30 minutes before recording. Recordings were performed in carbogenated external recording ACSF ($32.7 \pm 0.1^\circ\text{C}$) containing (in mM): 125 NaCl, 25 NaHCO_3 , 1.25 NaH_2PO_4 , 2.5 KCl, 1 $\text{MgCl}_2 \cdot 6\text{H}_2\text{O}$, 2 $\text{CaCl}_2 \cdot 2\text{H}_2\text{O}$ and 25 Glucose. MLIs and PCs of folia IV/V were targeted for recording by IR-DIC, or epifluorescence stimulated by a CoolLED pE-4000, detected via a SciCam Pro on a SliceScope Pro 6000-based rig (Scientifica). Recording electrodes were pulled (Narishige, PC-100) from standard-wall borosilicate glass capillary tubing (G150F-4, Warner

Instruments) and had 5.1 ± 0.08 and 2.8 ± 0.02 M Ω tip resistance for MLIs and PCs respectively. Spontaneous Inhibitory Postsynaptic Currents (sIPSCs) and Miniature Inhibitory Postsynaptic Currents (mIPSC) were recorded with an intracellular solution containing (in mM): 140 CsCl, 4 NaCl, 0.5 CaCl₂·2H₂O, 10 HEPES, 5 EGTA, 2 Mg-ATP, and 0.4 Na-GTP, 2 QX-314. For action potential recordings and for Miniature Excitatory Postsynaptic Currents (mEPSCs), the intracellular solution contained (in mM): 140 K-gluconate, 10 KCl, 1 MgCl₂, 10 HEPES, 0.02 EGTA, 3 Mg-ATP, and 0.5 Na-GTP as described previously [33]. The internal pipette solution pH was adjusted to 7.35 with CsOH for IPSCs and mIPSCs, and with KOH for mEPSCs and action potentials, while for all the osmolarity was adjusted to 300 mOsmolL⁻¹ with sucrose. In whole-cell voltage clamp mode PCs were held at -70 mV; to isolate sIPSCs, CNQX or NBQX (10 μ M) and D-AP5 (50 μ M) were added to the recording solution and mIPSCs recordings additionally included 1 μ M tetrodotoxin (TTX). To record mEPSCs, 1 μ M TTX and 50 μ M picrotoxin was added to extracellular solution. Action potentials were recorded in MLIs within the middle third of the molecular layer; spontaneous action potentials were recorded in I=0 mode, or action potentials were evoked by depolarizing current injection in 600 ms steps of 10 pA, from 0 to 150 pA, with a 7 second inter-sweep interval. For paired pulse, current ranging from 150 uA to 250 uA was delivered by concentric bipolar stimulating electrode in the molecular layer. Stimulus duration was 50 μ S, and ISI was 50 ms. For each cell, 10 sweeps were recorded with 10 S inter-sweep interval. A square-wave voltage stimulation pulse was utilized to determine input resistance and cell capacitance. Purkinje Cells with an access resistance of 10-20 (15.9 ± 0.5), or MLIs with an access resistance <30 (23.6 ± 0.6) M Ω were considered for recording. Recordings with >20% change in series resistance were excluded from analysis. Signals were acquired at 10 KHz with a low-noise data acquisition system (Digidata 1550B) and a Multiclamp700-A amplifier and were analyzed using pClamp11.1 (Molecular Devices) after low pass Bessel (8-pole) filtration (3dB cut off, filter 1 KHz). The minimum amplitude threshold for detecting IPSCs and EPSCs was 15 pA; for mIPSCs and mEPSCs the cutoff was 8 pA. For determining frequency and amplitude, individual events longer than 1 ms were included while overlapping events were manually rejected from analysis. Inhibitory charge is reported as the per-cell sum over the recording epoch of the area under the curve for all pharmacologically resolved inhibitory events. For the analysis of minis, both mIPSCs and mEPSCs with over 8 pA amplitude and longer than 1 ms duration were included while overlapping events were rejected from analysis; also rejected from analysis was any miniature event for which amplitude, rise, and decay metrics were not all available.

Software

Microscopic image processing was conducted via FIJI/ImageJ, electrophysiological data was analyzed by pClamp11.1, statistical analyses were conducted via GraphPad Prism 9, and Figures were created with BioRender, PowerPoint, and GraphPad Prism 9.

Results

We generated mice in which Kit exon 4 is flanked by LoxP sites (Kit tm1c); Kit gene modifications are illustrated in **Figure 1C, D**. Kit tm1c homozygous Control animals had normal appearance, sex ratios, and reproductive success. Kit is abundantly expressed in parvalbumin positive GABAergic interneurons in the molecular layer of the cerebellar cortex (MLIs), whereas Kit Ligand (KL) is expressed by Purkinje cells (PCs) (**Figure 1A, B**). To determine if Kit influences synapse function, we conditionally knocked out Kit from MLIs and assessed the MLI:PC synapse. Pax2 is a transcription factor expressed early in the lineage of GABAergic interneurons of the cerebellum [34]; a Pax2-Cre transgene enables embryonic recombination [35, 36]. We generated Kit tm1c homozygous litters of which nominally half were hemizygous for Pax2 Cre (Kit KO) and half were not (Control). We produced Control and Kit KO animals in normal sex and genotype ratios. As expected for the C57Bl6/J background, Control littermates had dark coat and eyes, but littermate Kit KO animals had white whiskers, white fur with variable pigmented patches, and black eyes;

example littermates **Figure 1E** [↗](#). Given Pax2 expression in melanocytes [[37](#) [↗](#)] and the role of Kit in melanogenesis (Reviewed in [[38](#) [↗](#), [39](#) [↗](#)]), the pigmentation phenotype provided gross confirmation of conditional Kit KO. We thus confirmed that cerebella of Kit KO animals were Kit depleted. By immunohistochemistry in Control animals, we recapitulated the known pattern of Kit immunoreactivity in the parvalbumin positive MLIs of the cerebellar cortex (Control, **1F and Inset**). In contrast, a sex-matched Kit KO littermate demonstrated loss of cerebellar Kit immunoreactivity (Kit KO, **1F and Inset**). In data not shown, we confirmed that both mGlu1/2 and neurogranin positive cerebellar Golgi cells (which share the MLI Pax2+ lineage, and of which some are transiently Kit positive) were still present in the Kit KO condition [[34](#) [↗](#), [40](#) [↗](#)-[42](#) [↗](#)]. By Western blot of cerebellar lysates from Control animals, Kit resolved as a major band at ~120 kD, but in Kit KO littermates, Kit immunoreactivity was lost; GAPDH as loading control was equivalent, as was parvalbumin (which marks mature MLIs and PCs) **Figure 1G** [↗](#).

Having validated that Kit KO animals indeed lacked cerebellar Kit, we then assessed the functional impact. We compared spontaneous GABAergic inhibitory post synaptic currents (sIPSC) in PCs of acute slices generated from ~P34 Control and Kit KO animals, schema **Figure 2A** [↗](#), example traces **Figure 2B** [↗](#). Kit KO was associated with a significant change in the distribution of sIPSC event amplitudes (**Figure 2C** [↗](#)). For each PC of Control or Kit KO conditions, we calculated the average sIPSC event frequency and amplitude, as well as total inhibitory charge transfer over the recording epoch. We determined there was a significant decrease in sIPSC frequency (**Figure 2D** [↗](#)) and a less severe decrease of sIPSC amplitude and inhibitory charge. This reduced inhibition did not produce obvious impacts to spontaneous PC firing dynamics: we determined (in 29 Control vs 22 Kit KO cells) that PC membrane potential and membrane resistivity were not significantly different, and that per cell average: spontaneous action potential frequency, interspike interval (ISI), and ISI CV2 were not significantly different, despite some difference in the distribution of individual ISI across genotypes. (**Figure S6** [↗](#)). Though circuit consequences of the Kit KO mediated PC disinhibition were thus not immediately apparent, the reduced sIPSC frequency in Kit KO was not associated with changes in the density or distribution of MLIs or in the thickness of the molecular layer (**Figure S2** [↗](#)).

Since the number and distribution of MLIs were normal in Kit KO, we sought to determine if the reduced PC inhibition was related to altered MLI physiology (Schema, **Figure S3A** [↗](#)). However, capacitance, input resistance, and spontaneous or evoked MLI action potential frequency was not different between Control and Kit KO (**Figure S3B-E** [↗](#)). Since MLIs numbers, distribution, and firing were apparently normal in Kit KO, we sought to determine if there were defects in evoked neurotransmitter release. Direct electrode stimulation of the outer or inner molecular layer in a paired-pulse paradigm (Schema, **Figure S3F,J** [↗](#); example traces **Figure G,K**) evoked IPSCs of equivalent mean amplitude in PCs from Control and Kit KO (**Figure S3H,L** [↗](#)), and we detected no difference in the paired pulse ratio between conditions (**Figure S3I,M** [↗](#)). These data suggest that direct stimulation can evoke a similar maximum of release probability between Control and Kit KO conditions. We therefore investigated markers of the MLI:PC synapses to determine if they were altered.

The density and average size of GABAergic synapses onto PCs (triple positive VGAT, Gephyrin, and Calbindin puncta in the molecular layer) was not reduced by Kit KO (example immunofluorescence, **Figure S4A** [↗](#), Quantification **S4B,C** [↗](#)). MLI axon terminals contribute not just to individual axo-dendritic synaptic puncta, but also to interdigitated MLI axon collaterals around the soma and initial axon segment of PCs, forming “pincheaux” structures. By parvalbumin immunoreactivity, these structures were preserved but smaller in Kit KO (arrowheads **Figure S4C** [↗](#)), and this was confirmed by decreased Kv1.2 (**Figure S4D** [↗](#)) and PSD-95 (**Figure S4E** [↗](#)). As PSD-95 immunoreactivity faithfully follows multiple markers of pincheaux size [[43](#) [↗](#)], we quantified PSD-95 immunoreactive pincheau area and we determined that pincheaux size was

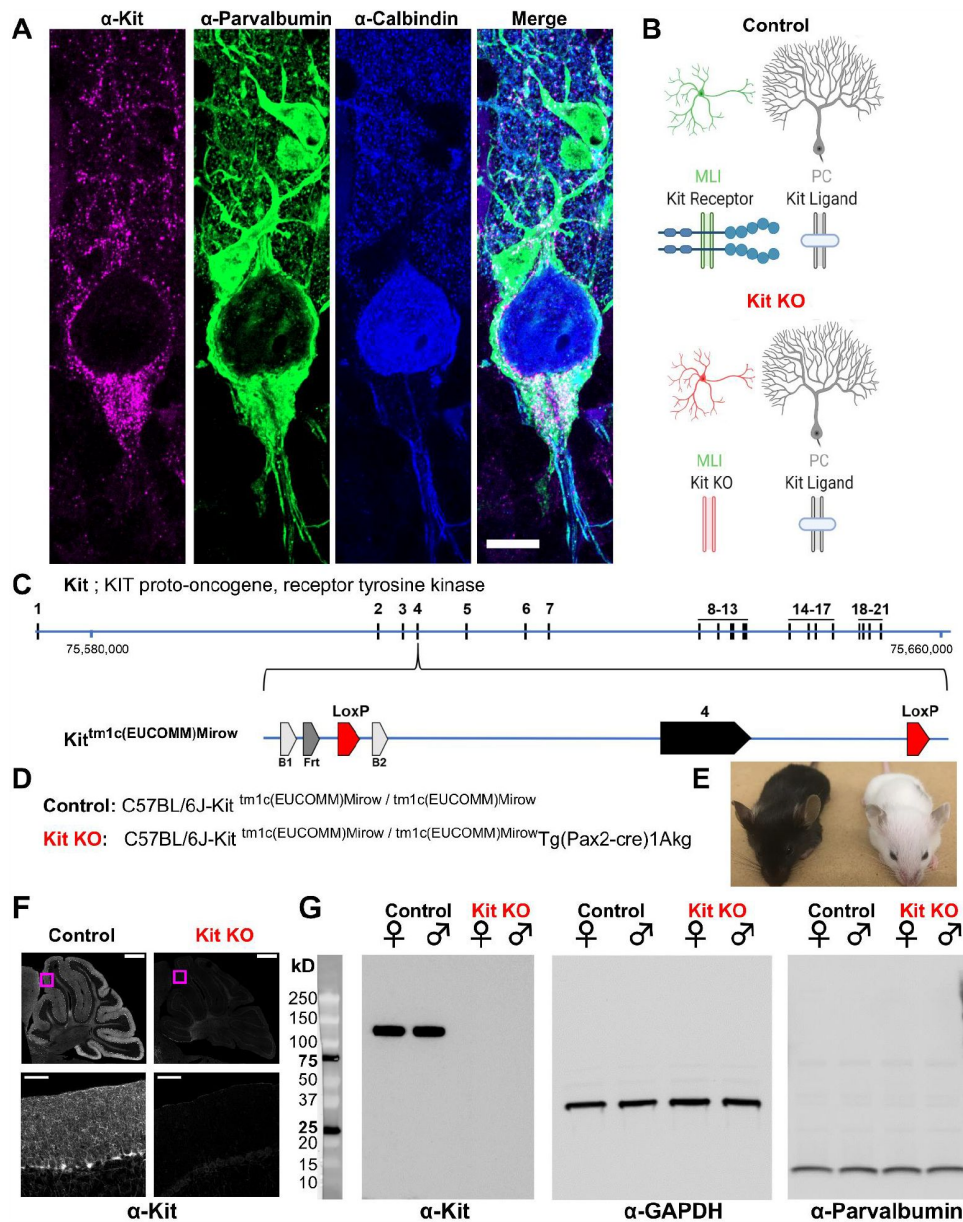


Figure 1

Design and validation of a Kit conditional knockout mouse.

(A, B) Kit receptor tyrosine kinase (Kit) is enriched in parvalbumin positive GABAergic interneurons of the molecular layer (i.e. basket and stellate cells, MLIs) of the cerebellar cortex, where they synapse onto each other and onto Purkinje cells (PCs, Calbindin+), which express Kit Ligand (KL). Scale bar 10 microns. Expression pattern schematized in B, Control.

(C) In humans and mice, Kit is encoded by up to 21 exons, which in mouse is encoded on the plus strand of chromosome 5 at 75,735,647-75,817,382 bp. We generated a Kit conditional knockout mouse in which Kit Exon 4 is floxed, flanked by LoxP sites.

(D) We generated Control mice homozygous for the Kit floxed allele *Kit^{tm1c(EUCOMM)Mirow}*, which varied in Pax2-Cre1Akg transgene status, with the goal of depleting Kit from MLIs in embryonic development.

(E) Pax2 Cre mediated Kit KO mice were notably hypopigmented in hair and whiskers, though not eyes.

(F) Confocal microscopy of Kit immunoreactivity in cerebella from age and sex matched Control and Kit KO littermates demonstrates the established enrichment of Kit in the molecular layer of the Control cerebellar cortex, and its loss in Kit KO. Scale Bar 500 microns top row, 50 microns inset.

(G) Utilizing a distinct assay and different primary antibody, we confirm the detection of Kit immunoreactivity in Controls, and its loss in Kit KO littermates of either sex by Western Blot of total protein lysates of cerebella. We affirmed equivalent protein loading by GAPDH and parvalbumin.

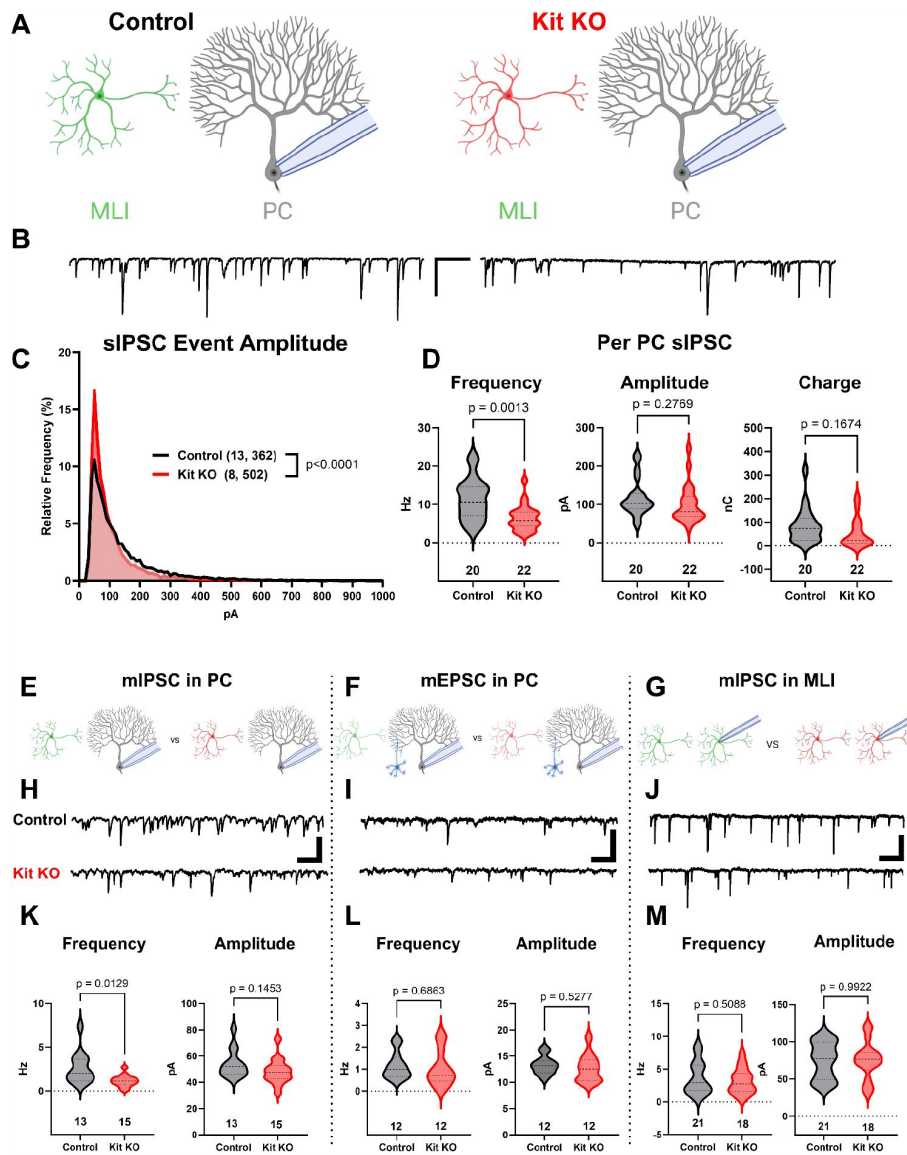


Figure 2

The knockout of Kit from Cerebellar Cortex Interneurons Impairs Inhibition of Purkinje Cells. 419

(A, B) Experimental schema and example traces of spontaneous inhibitory postsynaptic currents in Purkinje Cells (PCs) from Control animals or from those with Kit KO from cerebellar cortex molecular layer interneurons (MLIs). Scale bar is 500 ms x 100 pA.

(C) A frequency distribution plot for individual sIPSC event amplitudes recorded in PCs as in A,B. A KS test reveals a significant difference in the distribution of these event amplitudes; $p < 0.0001$, n in chart.

(D) For each PC, the average sIPSC Frequency and Amplitude, and the total Inhibitory Charge transfer, was determined. There was a significant ~50% decrease in sIPSC frequency, but the decrease in Amplitude or Charge transfer was not significant.

(E-G) Experimental schema: In separate experiments, we recorded miniature postsynaptic currents from PCs or from MLIs in Control and in Kit KO animals.

(H) Example traces of mIPSCs or (I) mEPSCs recorded in PCs, and example traces of mIPSC in MLIs, all from Control or from Kit KO animals. Scale for H and J is 50 pA, 25 pA for I, all 500 ms.

(K-M) Analysis of per cell average miniature event Frequency and Amplitude revealed that Kit KO significantly reduced mIPSC frequency, but not amplitude, in PCs by >50%, $p = 0.013$. mEPSCs in PCs and mIPSC in MLIs were not significantly different between Control and Kit KO.

n in charts, refers to the number of cells. Error bars are SEM. p-values were calculated by a two-tailed t-test, with Welch's correction as needed.

decreased by ~50% in Kit KO (26 Control vs 43 Kit KO pinceau from n of 5 Control vs 8 Kit KO animals, **Figure S4F**). These results suggested that Kit KO MLIs may have defects in physical and/or functional maturation of synapses onto PCs.

To evaluate the number of functional GABAergic synapses, we analyzed miniature synaptic currents in acute cerebellar slices, (schema **Figure 2 E, F, G**; example traces **Figure 2 H, I, J**). In PCs of Kit KO, there was a significant ~50% reduction in the average frequency, but not amplitude, of mIPSCs (**Figure 2K**). In contrast, the average frequency and amplitude of mEPSCs in PCs from Control and Kit KO did not differ (**Figure 2L**). These data suggested that Kit KO impaired the MLI:PC synapse but did not rule out a general defect in MLI synapse function. As MLIs synapse not just onto PCs, but also onto other MLIs, we evaluated mIPSCs in MLIs. Mean mIPSC frequency and amplitude in MLIs was unchanged between Control and Kit KO (**Figure 2M**). Therefore, embryonic MLI Kit KO was associated with a specific defect in the number or proportion of functional GABAergic synapses onto PCs. As MLI Kit and PC KL expression is maintained postnatally, we hypothesized that postnatal postsynaptic PC KL KO would phenocopy embryonic presynaptic MLI Kit KO.

We utilized previously described KL floxed [23] and Pcp2-Cre [24] strains to yield mice with Control or KL KO PCs (Schema **Figure 3A**). We confirmed depletion of cerebellar KL transcripts by rtPCR in data not shown [23], and we confirmed that PC KL KO did not grossly disrupt the pattern of Kit immunoreactivity. Patch clamp of PCs in acute slices revealed that PC KL KO produced significant differences in the distribution of sIPSC event amplitudes (Example traces **Figure 3B**, **Figure 3C**). PC KL KO reduced the average sIPSC frequency and amplitude, as well as the total inhibitory charge transfer (“Charge”) recorded in PCs (**Figure 3D**), without changes to PC capacitance or membrane resistance. The phenotype was specific to GABAergic synapses: there was a substantial reduction in the frequency but not the amplitude of mIPSC events in PCs (**Figure 3E**). As with Kit KO, we detected no decrease in the per-animal average size or density of triple positive VGAT/Gephyrin/Calbindin synaptic puncta in the molecular layer (n=4 Control vs 4 KL KO animals, mean area 0.249 vs 0.286 μm^2 , p=.1962; mean density 0.045 vs 0.046 per μm^2 , p=.9658), Not Illustrated). We further detected no difference either in PDS-95+ pinceau area (49 Control vs 48 KL KO pinceaux from n=4 Control vs 4 KL KO animals, mean area 57.93 vs 53.37 μm^2 p=.6036, Not Illustrated). Thus, as with Kit embryonic Kit KO, postnatal KL KO apparently reduced the proportion of functional, if not the absolute structural total, of GABAergic synapse sites upon PCs. In contrast to this impact on GABAergic synapses, the frequency and amplitude of mEPSCs in KL KO PCs was not different vs Controls (**Figure 3F**). In data not shown, a KS test revealed a significant difference in the individual mEPSC event amplitude distribution (p=0.0002, n=1196 Control vs 1244 KL KO), however the mean mEPSC amplitude was within 1% between conditions. Similarly, a KS test of mIPSC event amplitudes revealed that the mean mIPSC amplitude was ~10% greater in PC KL KO than in Control (p<0.0001, n=5996 Control vs 3958 KL KO). It is therefore unlikely that decreased event amplitude contributed to the specific and robust >50% decrease in mIPSC frequency detected in PC KL KO. Thus, as with MLI Kit KO, PC KL KO specifically reduced synaptic inhibition of PCs.

Recombination by Pcp2 Cre begins at ~P7 [24], whereas Pax2 Cre recombination occurs at ~E15 [21, 34]. Our results thus suggest that continued expression of the KL-Kit dyad sustains inhibitory drive to PCs. To test this hypothesis (and to avoid transformative effects of Kit overexpression), we tuned KL postnatal expression *in vivo*.

To determine if acute focal manipulations in KL modulate PC inhibition, we injected replication-defective viruses leveraging the PC-specific L7.6 promoter [32] to express Cre in KL floxed animals, and we identified Cre-positive KL KO PCs by mCherry expression (Schema **Figure 4A**, Example transduction, **Figure S5A-C, E-G**). Injections were at P7, P18, or P56; acute slices were generated 2-3 weeks after injections. In the P7 neonatal animals we utilized lentivirus owing to its reduced spread vs AAV particles, which were used for P18 and P56. Patch-clamp recordings in

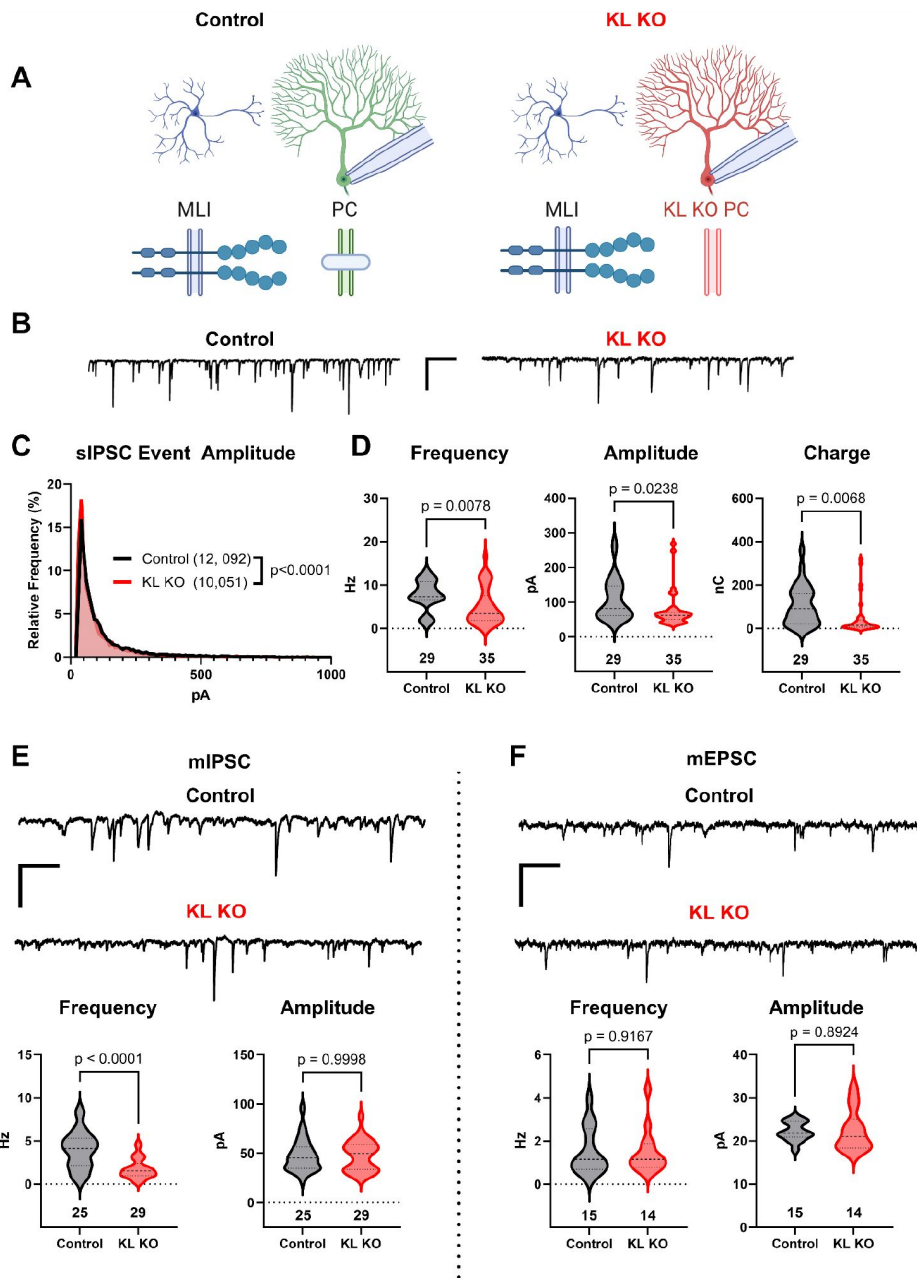


Figure 3

Knockout of Kit Ligand from Purkinje Cells decreases the inhibitory input they receive.

(A, B) Experimental schema and example traces of inhibitory postsynaptic currents detected in Purkinje Cells (PCs) from Control animals or from those with Kit Ligand knockout (KL KO) accomplished by a *Pcp2-Cre* x KL floxed strategy. Scale bar is 500 ms x 100 pA.

(C) A frequency distribution plot for individual sIPSC event amplitudes recorded in PCs as in A, B. A KS test reveals a significant difference in the distribution of these event amplitudes; $p < 0.0001$, n in chart.

(D) For each PC, the average sIPSC Frequency and Amplitude, and the total inhibitory Charge transfer, was determined. There was a significant ~40% decrease in sIPSC Frequency, Amplitude, and Charge transferred to KL KO PCs.

(E, F) The average mIPSC recorded in PC KL KO vs Control PCs had a >50% decreased Frequency $p < 0.0001$ without a corresponding decrease in Amplitude. The average mEPSC Frequency and Amplitude recorded in separate PCs did not differ between Control and KL KO. Scale bar is 500 ms x 100 pA for mIPSC, 500 ms x 50 pA for mEPSC.

n in charts refers to number of cells. Error bars are SEM. p-values were calculated by a two-tailed t-test, with Welch's correction as needed.

areas of sparse infection revealed that regardless of when KL was depleted, PC KL KO reduced PC sIPSC frequency and inhibitory charge transferred (P7, P18, and P56 in **Figure S5 D, H, I**; P18 injections **Figure 4 B, C, D**). We next examined the effects of PC KL over-expression using a complementary strategy. We co-injected L7.6 Cre AAV with AAV encoding EF1 α driven Cre-on mCherry and the membrane bound isoform of mouse KL (mKL2) via a T2A element to produce PC KL overexpression (OX) (Schema **Figure 4E**). Whether at P18 (shown) or P56 (not shown), KL OX PCs had increased sIPSC frequency, amplitude, and inhibitory charge transferred, compared to nearby Control PCs (**Figure 4F, G, H**). We noted that Control PCs from the PC KL KO paradigm received a similar degree of inhibition (frequency, amplitude, charge) as did PCs from Sham injections. In contrast, while the KL OX PCs received elevated GABAergic input compared to their adjacent Control PCs, the (KL OX) relative local increase in inhibitory drive was not beyond the level of inhibition recorded in PCs from separate Sham animals (**Figure 4F, G, H**). That is, the local gain in synaptic input to KL OX PCs appears to come at the expense of decreasing inhibition to nearby Control PCs.

Discussion

For genes essential to survival or reproduction, germline knockout strategies are not feasible for evaluating postnatal physiology. Among such genes, *Kit* is an example of a highly pleiotropic gene, and so the interpretation of global hypomorphs is challenging and the recombination of conditional alleles outside of desired tissues can lead to lethal or sterile phenotypes. By generating a conditional knockout mouse, we were able to produce viable animals with *Kit* depleted from the cerebellum to reveal a role in synapse function.

MLI number, distribution, action potential firing, and the density of GABAergic synaptic puncta onto PCs, are all apparently normal in MLI *Kit* KO. These data suggest that while MLI axon terminals are present in *Kit* KO, they may be less functional. An increased failure rate between action potential generation and neurotransmitter release would be consistent with the normal firing frequency and synapse puncta density but decreased sIPSC and mIPSC frequency observed. Under the PPR paradigm, the apparently equivalent evoked responses may be due to direct stimulation of axon terminals and/or simultaneous recruitment of multiple MLIs.

Kit KO most directly impacts the MLI:PC synapse, based on seemingly normal miniature events for parallel fiber: PC synapses (mEPSC in PC) and MLI:MLI (mIPSC in MLI) synapses. This is perhaps expected given the cell type specific expression of KL by PCs and *Kit* by MLIs, however, it is a critical distinction as *Cerebellins* [44] and *Calsystenin* [45] impact multiple forms of synaptic input to PCs. It will be informative to determine if the residual inhibitory drive to PCs observed in MLI *Kit* KO or PC KL KO comes from PC axon collaterals [46-49] whose input we might expect to be preserved if KL-*Kit* functions primarily to mediate connectivity between different cell types, or perhaps from a subtype of interneuron not dependent upon *Kit* signaling. This distinction is further relevant since our histological analysis of synaptic puncta does not resolve between MLI:PC and PC:PC synapses, the relative balance of which may be altered by either KL or *Kit* manipulations. Indeed, future studies of the role of KL-*Kit* on PC-PC connectivity may inform how PC KL OX can apparently weaken inhibition to adjacent PCs: this may occur through the reduction of inhibitory drive from KL OX PCs to adjacent control PCs. An alternative, and not mutually exclusive possibility is that PC KL OX excessively potentiates MLI *Kit* to enhance MLI:MLI inhibition, reducing the inhibitory output surrounding MLIs can provide to control PCs.

Though such important nuances of the circuit mechanisms remain to be elucidated, our results demonstrate that the KL-*Kit* axis, from embryonic development through young adulthood, can alter GABAergic drive to PCs. These results suggest that KL-*Kit* may be necessary to maintain, and perhaps capable of modulating, MLI:PC GABAergic inhibition in the adult cerebellum. As each MLI (e.g. basket cell) has axon collaterals that can target multiple PCs, and as each PC can receive input

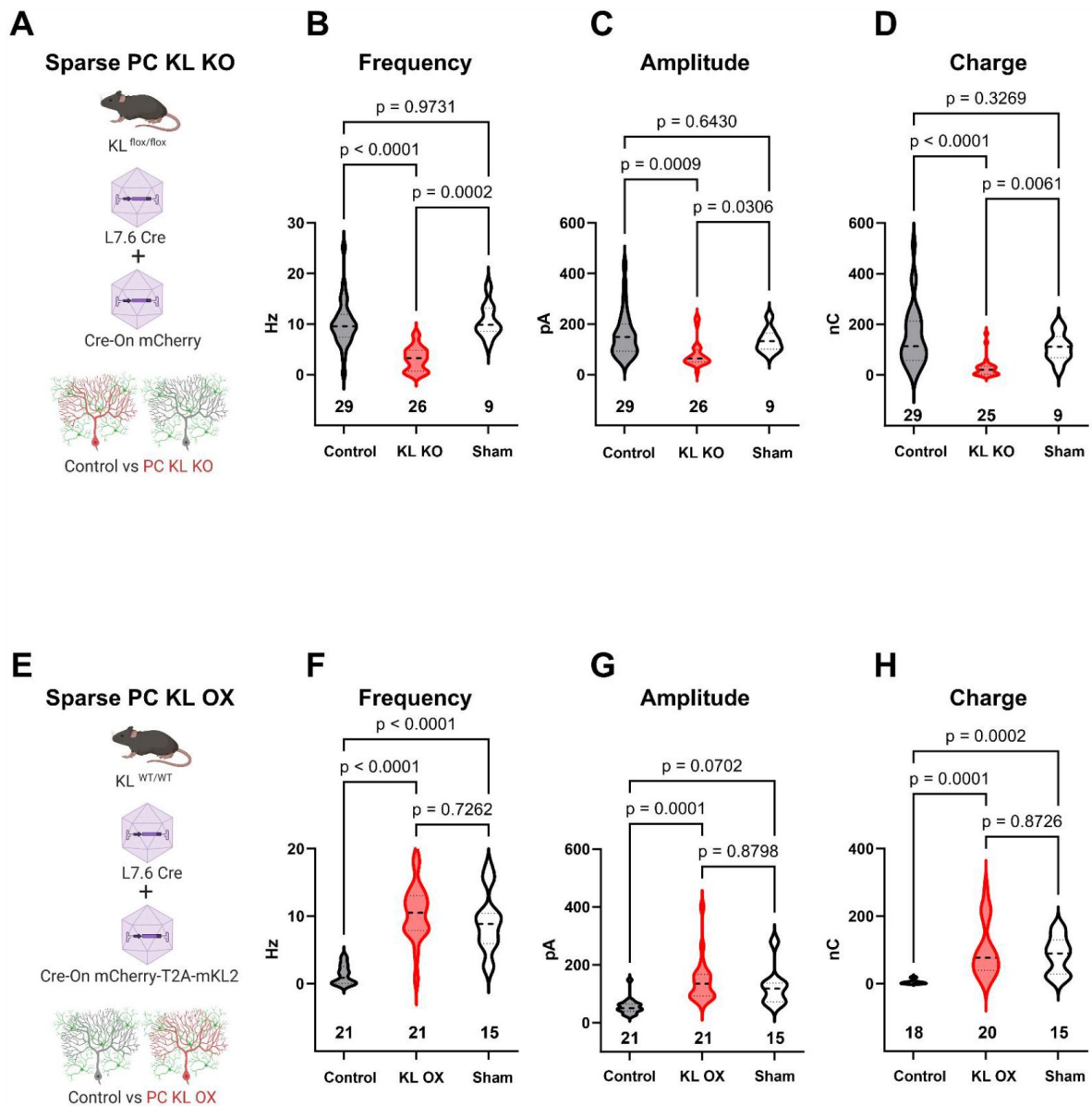


Figure 4.

Local levels of Kit Ligand influence the inhibition Purkinje cells receive.

(A) To accomplish *in vivo* Control and sparse Kit Ligand Knockout (KL KO) Purkinje Cells (PCs), an AAV encoding Cre under the PC specific L7.6 promoter was co-injected with an AAV encoding a Cre-On mCherry cassette under the Ef1 α promoter.

(B, C, D) In animals injected at P18, PC KL KO neurons demonstrated a ~70% decrease in sIPSC event frequency compared to adjacent Control PCs ($p < 0.0001$) or PCs recorded from Sham control animals ($p = 0.0002$). Control vs Sham sIPSC frequency was not significantly different. The same pattern was found for both mean sIPSC Amplitude (C) and for total inhibitory Charge transferred (D).

(E) To accomplish *in vivo* Control and sparse Kit Ligand overexpressing (KL OX) PCs, the L7.6 Cre AAV was co-injected with AAV expressing mCherry and (T2A) murine Kit Ligand isoform 2 under the Ef1 α promoter.

(F, G, H) In animals injected at P18, PC KL OX neurons demonstrated an ~8-fold increase in sIPSC Frequency vs neighboring Control PCs ($p < 0.0001$). The frequency of sIPSC events in KL OX PCs was not significantly different from PCs recorded in different Sham animals; this Sham PC sIPSC frequency (while comparable across studies) was 7-fold higher than Control PCs within the KL OX experimental animals ($p < 0.0001$). A similar pattern was found for sIPSC amplitude (G) and for total inhibitory Charge transferred (H).

n in charts, refers to number of cells. Error bars are SEM. p-values were calculated by Brown-Forsythe ANOVA test with Dunnett's T3 multiple comparisons test.

from multiple MLIs, it is interesting to speculate that dynamics (e.g. in the expression or shedding) of KL may act through presynaptic Kit to tune the degree of convergent MLI:PC inhibitory drive. This would complement existing forms of modulation at the MLI:PC synapse, such as those dependent on other PC derived signaling molecules, like endocannabinoids [50-52] or peptides like secretin [53, 54] and CR [55]. The physiology of PCs, and the structure of MLI:PC inhibition, also varies over zones such as those identified by Zebrin-II and PLC β 4 [56-60]; whether there is functional variation in KL or Kit expression, signaling, or dependency, remains to be determined. Though we have demonstrated a role in synaptic GABAergic inhibition, it is currently unknown whether Kit signaling also plays a role in other forms of inhibition in the cerebellar cortex, such as MLI:MLI gap-junctions, or MLI:PC ephaptic coupling. The latter may be suggested by the Kit KO mediated reduction in Kv1.1/Kv.12 and PSD-95 immunoreactivity.

While KL-Kit clearly influences synaptic function, we do not yet know the molecular mechanisms involved. Kit is a receptor tyrosine kinase that can activate multiple downstream effectors including Src family kinases, PLC, PI3K/mTOR, and the MAPK pathway, the latter two notable here for their shared affiliation with synapse phenotypes and autism spectrum disorder. Investigation of the interactome of Kit under basal and KL manipulated conditions may inform the receptor kinase cascades through which Kit signaling sustains synaptic function. It is also plausible that trans-cellular interactions between KL and Kit may function in a kinase-independent, cell adhesion molecule modality [61, 62]. There is a substantial literature illustrating the importance of adhesion molecules in the organization and maintenance of MLI:PC inhibition, such as neurexins/neuroligins, dystrophin/dystroglycan, semaphorins, and neurofascins [44, 45, 63-67]. Much of what is understood about these molecules in the maintenance of PC inhibition is revealed by post-synaptic phenotypes; that is, cis- and trans-interacting proteins that, via gephyrin, maintain the organization of PC GABA_A receptors. It is notable therefore that MLI Kit or PC KL KO has a more predominant effect on mIPSC frequency than on amplitude, suggesting a presynaptic phenotype.

Despite the reduced PC inhibition resulting from MLI Kit KO or from PC KL KO, we have not observed overt cerebellar signs (i.e., ataxia). We suspect that this is due to compensation. Even the developmental ablation of functional GABA_A channels in PCs does not produce overt motor signs, while adulthood ablation can [68]. Thus, we might unmask behavioral phenotypes if KL or Kit KO is delayed until adulthood. Consistent with the interpretation that developmental compensation may be involved, the impact of postnatal PC KL KO on inhibitory drive to PCs is more pronounced than embryonic MLI Kit KO. Beyond direct inhibition of PCs, MLI:PC GABAergic inhibition constrains granule cell mediated PC dendritic excitation and thus gates the conversion of PC LTD to LTP at the PF-PC synapse in motor learning [69, 70]. It is therefore possible that KL or Kit KO may only reveal phenotypes in motor learning (or other cerebellar-plasticity dependent) behaviors; speaking to the feasibility of this possibility, global hypomorphs for KL or Kit have altered hippocampal neurophysiology and learning performance on a Water Maze task [71-73]. Continuous expression of KL and Kit in specific neurons may thus reflect not only a role in the development (or maintenance) of synaptic function as suggested here, but also in the plastic modulation of synaptic strength.

Despite the importance of future works to determine molecular mechanisms and organismal consequences, our study is a discrete advance because it establishes that KL-Kit regulates mammalian central synapse function. Here, we demonstrate impacts at the mouse GABAergic MLI:PC synapse; however, Kit and KL exist in diverse organisms and neuronal populations including glutamatergic neurons of the hippocampus, and neurons in olfactory bulb, basal forebrain, and brainstem. It is therefore feasible that the synaptic phenotypes reported here reflect that KL-Kit is broadly capable of influencing connectivity.

Supplementary Information

Six Figures and Associated Legends

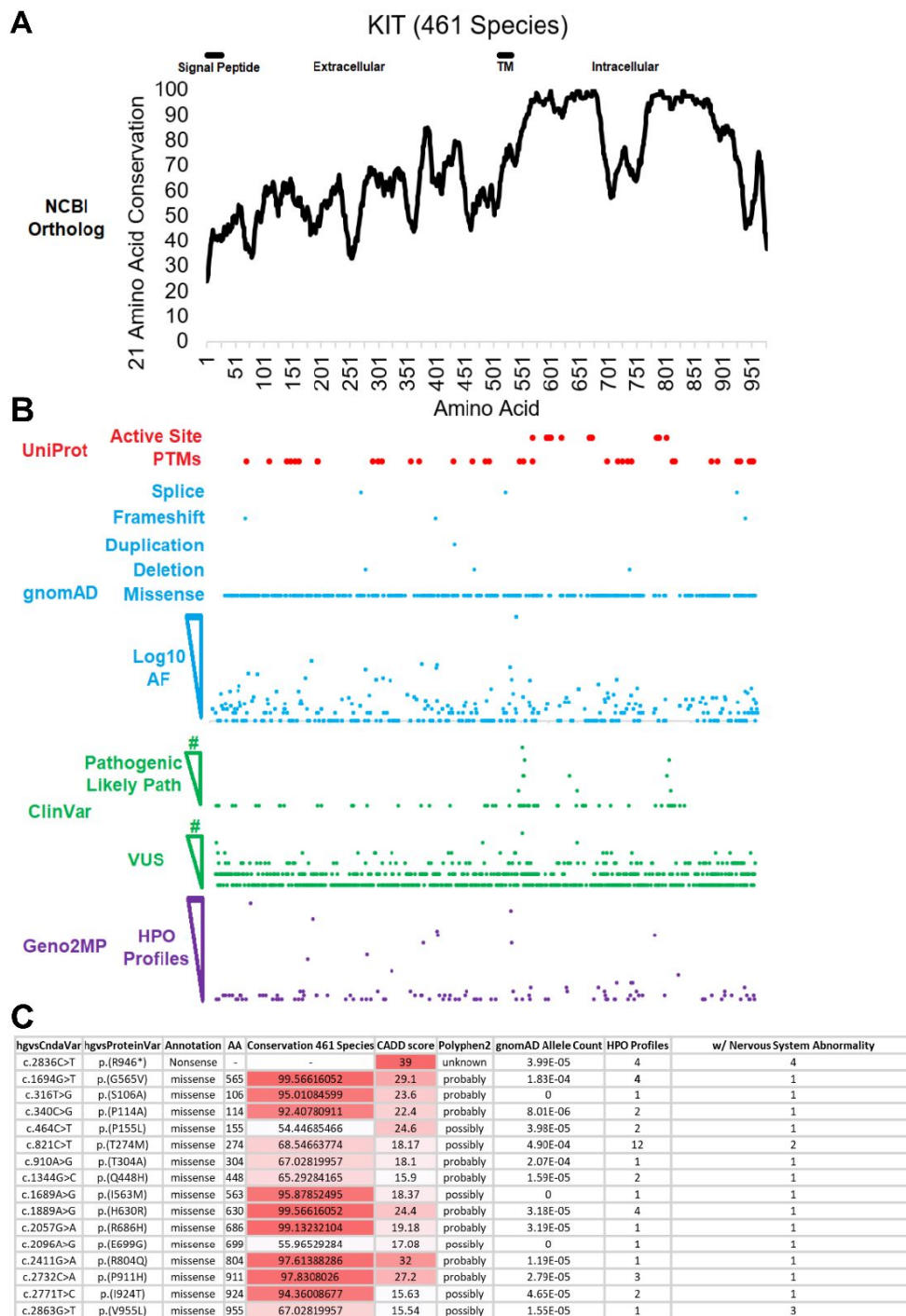


Figure S1

Kit receptor tyrosine kinase is a highly conserved gene affiliated with neurological impairment.

(A) KIT protein sequences were extracted from NCBI ortholog on March 2023 and aligned with MUSCLE. Conservation was placed on a 21 amino acid sliding window to calculate linear motifs. The intracellular domain possesses a split cytoplasmic kinase motif demonstrating high conservation across 461 species.

(B) Alignment of Active Site and Post-Translational Motif (PTMs) to Kit amino acid conservation and gnomAD, ClinVar, and Geno2MP human variants.

(C) Human Genome Variation Society annotations for human DNA and corresponding encoded amino acid changes affiliated with their mutational class (Annotation), Site (AA), and Conservation across 461 species. Combined Annotation Dependent Depletion (CADD) score for deleteriousness of SNV or indel variants. Polymorphism Phenotyping v2 (PolyPhen2) annotations predict impact of amino acid substitution on Kit structure function. Allele counts in Gnomad and the number of profiles in the Human Phenotype Ontology associated with Nervous System Abnormality.

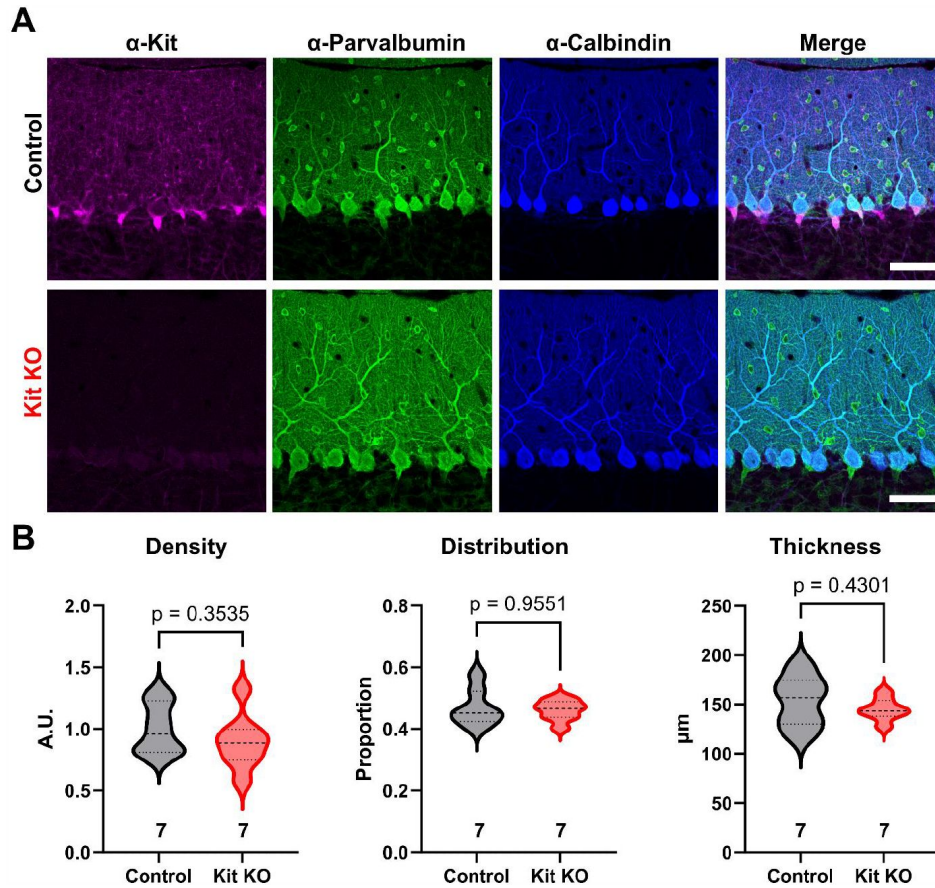


Figure S2

Kit knockout does not alter molecular layer interneuron number or distribution.

(A) Immunohistochemistry and confocal microscopy of Control and Kit KO mouse cerebellar cortex validates the normal enrichment and targeted depletion of Kit in Control and Kit KO animals respectively. Parvalbumin immunoreactivity is present in both Molecular Layer Interneurons and Purkinje Cells, while the latter is selectively Calbindin immunoreactive. Scale bar 80 microns.

(B) Quantification of the density of Parvalbumin positive and or Calbindin negative somas within the molecular layer reveals that the Density of MLIs is not reduced by Kit KO. Quantification of the average position of MLI somas between the basal (0) and distal (1) borders of the Molecular Layer reveals that the Control and Kit KO MLIs have comparable distributions within the molecular layer. Quantification of the thickness of the molecular layer reveals no significant difference between Control and Kit KO conditions.

p-values were calculated by a two-tailed t-test with Welch's correction as necessary, except for Distribution which utilized Mann-Whitney. N refers to the number of different animals whose comparable tissues were evaluated.

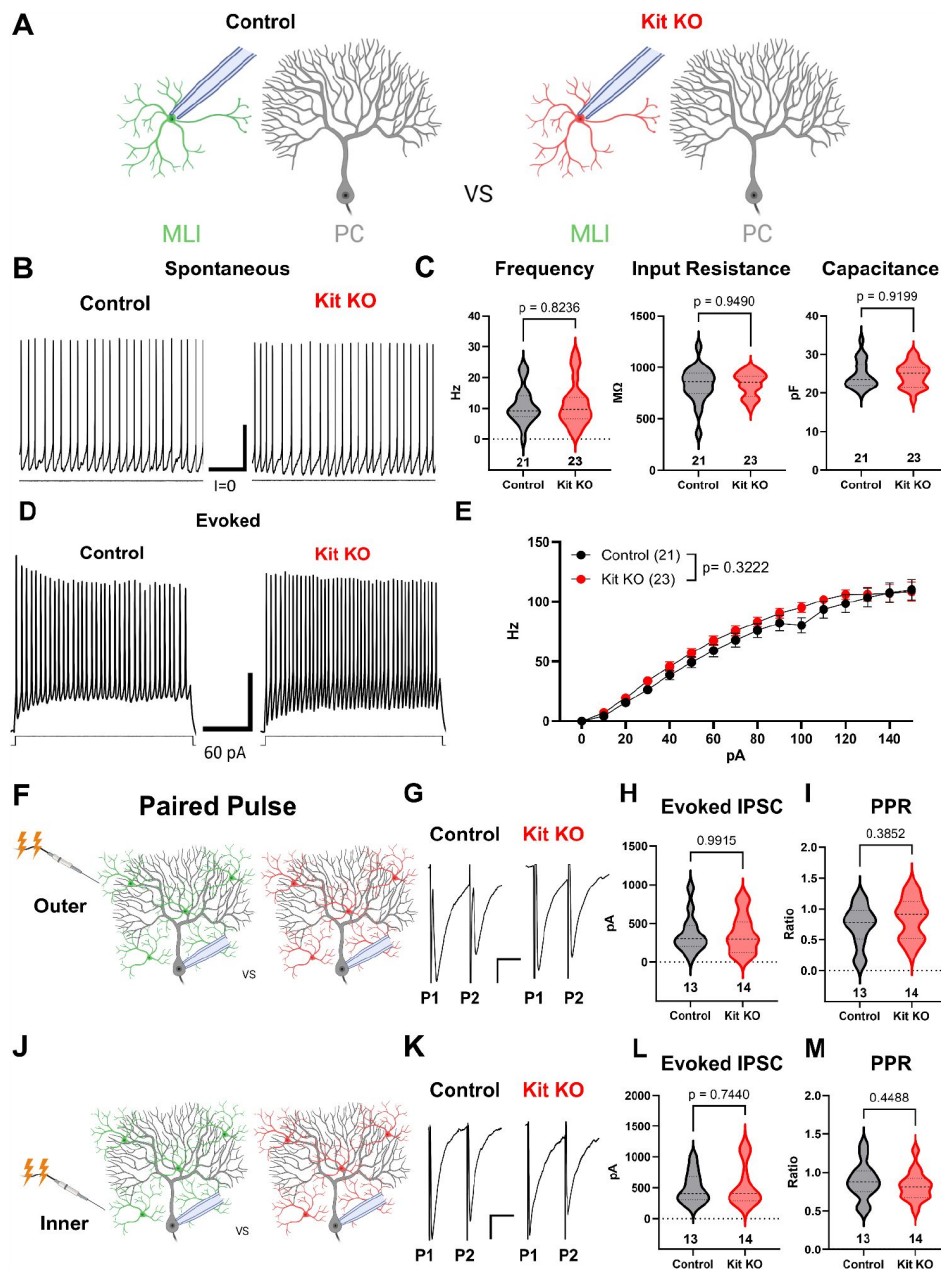


Figure S3

Kit knockout does not alter intrinsic properties of molecular layer interneurons.

(A) Experimental schema. Patch clamp recordings were performed on Molecular Layer Interneurons in acute cerebellar slice preparations from Control or from Kit KO animals.

(B,C) Patch clamp recordings of Spontaneous action potentials and intrinsic properties in Control and Kit KO MLIs revealed no significant difference in average firing Frequency, membrane Capacitance or Input Resistance. Scale bar 100 ms x 10mV.

(D, E) Current steps were injected into Control or Kit KO MLIs, example traces (D) and quantification (E) revealed no significant interaction of genotype and current on evoked mean firing Frequency. Scale bar 100 ms x 10mV

(F, J) Experimental schema. Paired pulses were delivered via stimulating electrode placed in the Outer or in the Inner molecular layer, and evoked Inhibitory Post Synaptic Currents were evaluated. Example Traces in G and K.

(H, I, L, M) The average amplitude of the first evoked inhibitory current, or the Paired Pulse Ratio, did not differ between Control and Kit KO, under either stimulation of the Outer or Inner molecular layer.

p-values were calculated by a two-tailed t-test with Welch's correction as necessary. n refers to the number of different recorded cells per condition.

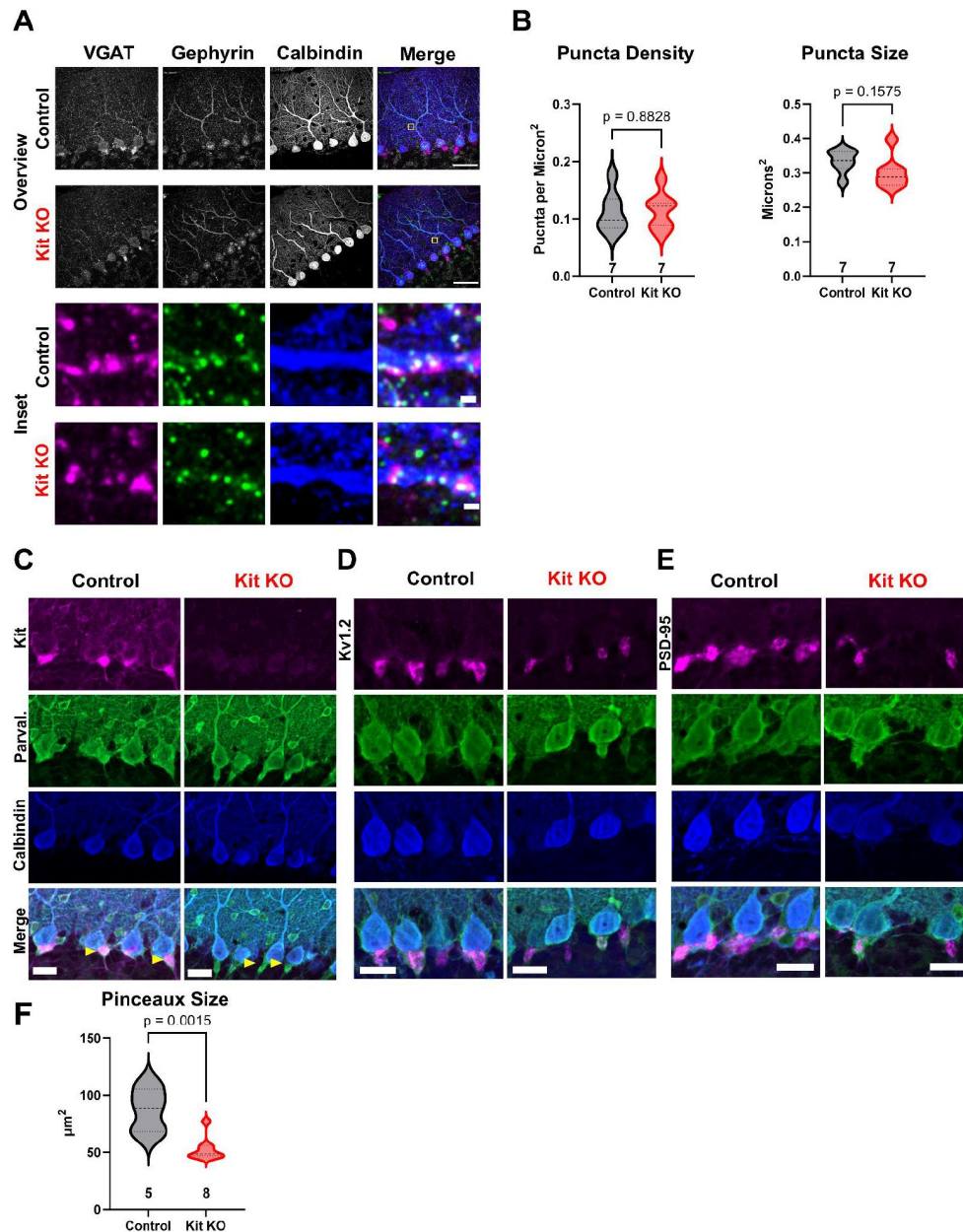


Figure S4

The impact of Kit knockout on the size of molecular layer interneuron synaptic structures.

(A) Immunohistochemistry and confocal microscopy of presynaptic (VGAT) and postsynaptic (Gephyrin) markers of GABAergic synapses onto Purkinje Cells (Calbindin), for both Control and Kit KO. An Inset from Control (Yellow Box, first Row Merge ROI), demonstrates example triple positive puncta. First two rows, scale bar 50 microns.

(B) Neither the average density nor the average size (per animal) of GABAergic synaptic puncta onto Purkinje Cells was significantly decreased by Kit KO.

(C, D, E) Immunohistochemistry and confocal microscopy of markers of the pinceau formation (of MLI axons onto PC soma and initial axon segments). For both Control and Kit KO, Calbindin and Parvalbumin immunoreactivity was determined in conjunction with pinceau markers Kit, Kv1.2, or PSD-95. As evidenced by Parvalbumin positive Calbindin negative pinceau structures in Kit KO in C, pinceau structures do still exist in Kit KO, though they appear smaller. This was affirmed by reduced area of Kv1.2 immunoreactivity, and by PSD-95 immunoreactivity, the latter of which is quantified in (F). Scale bars are 50 microns.

p-values were calculated by a two-tailed t-test with Welch's correction as necessary. n refers to the number of different animals per condition.

Virus Mediated PC KL KO sIPSC in PC

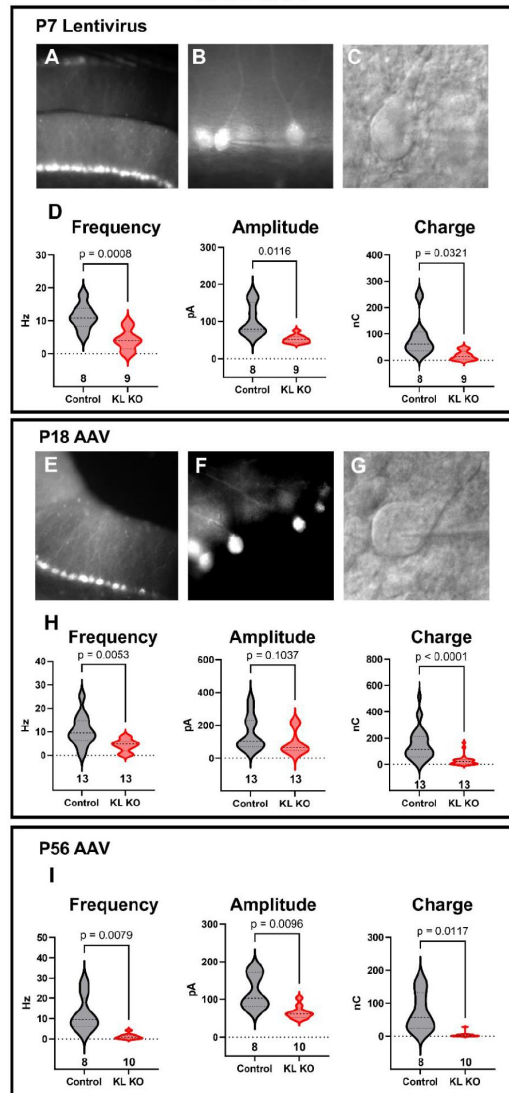


Figure S5

Sparse Acute Depletion of Kit Ligand Reduces GABAergic Input To Purkinje Cells.

(**A, B, C**) Lentivirus encoding mCherry-T2A-Cre under the Purkinje Cells specific promoter L7.6 was injected into postnatal day 7 mice homozygous for a Kit Ligand (KL) floxed allele at P7. Demonstrated in (**A**) is an area of direct hit and high transduction. (**B**) Areas with sparse PC transduction were used to record from KL KO or from uninfected adjacent Control PCs, with an example of an IR-DIC identified and patched PC (**C**).

(**D**). Analysis of the sIPSCs recorded from P7 Control or sparse KL KO PCs revealed that KL KO reduced both the mean frequency ($p=0.0008$) and amplitude ($p=0.012$) and the total inhibitory Charge transfer of GABAergic inhibitory currents in PCs by ~50%.

(**E, F, G**) AAV encoding Cre under the L7.6 promoter was co-injected with an AAV encoding Cre-On mCherry under the Ef1 α promoter into the cerebellum of postnatal day 18 or 56 KL floxed homozygous mice. Demonstrated in (**E**) is a direct hit with high transduction, areas as in (**F**) with sparse transduction were selected for recordings of mCherry positive KL KO PCs and adjacent uninfected Control PCs patched under IR-DIC (**G**).

(**H, I**). Analysis of the sIPSCs in Control and KL KO PCs at either P18 (**H**) or at P56 (**I**) revealed that mean sIPSC Frequency and Amplitude and total inhibitory Charge transferred were all markedly reduced by postnatal PC KL KO.

p-values were calculated by a two-tailed t-test with Welch's correction as necessary. N in columns refers to the number of different cells recorded.

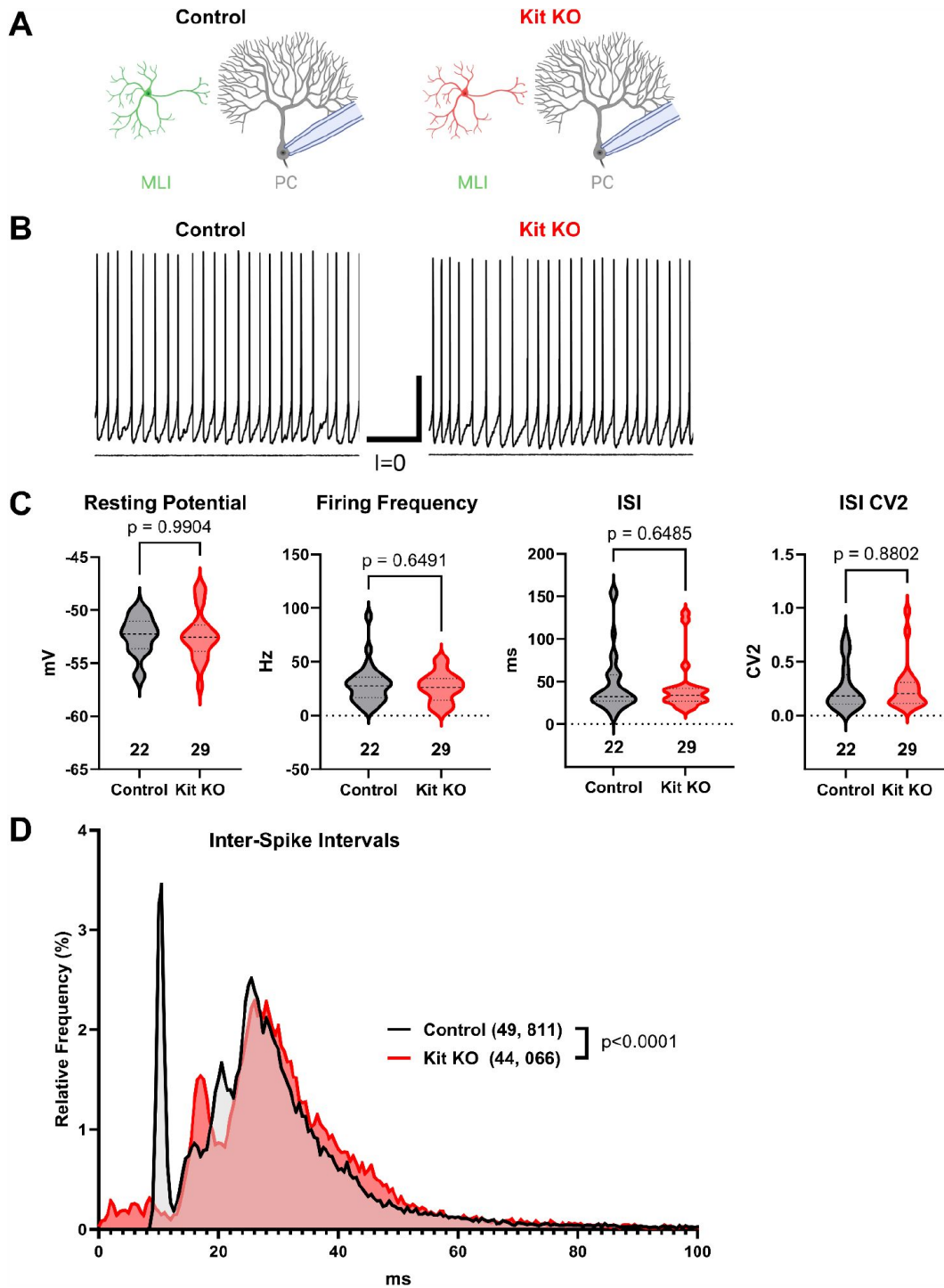


Figure S6.

Kit KO does not impact basal Purkinje Cell firing.

A) Experimental schema and **B)** example traces. Whole cell patch clamp recordings were made from Purkinje cells in acute cerebellar slices from Control or from Kit KO mice. Scale 250 ms x 20 mV.

(C) Analysis of PC resting membrane potential, spontaneous action potential firing frequency, average per cell Inter-Spike Interval, or per cell ISI CV2, revealed no significant differences between conditions. p values calculated by two-tailed t-test with Welch's correction as needed.

(D) A histogram and KS test of individual inter-spike intervals illustrates some differences in the distribution of PC spike timing in Kit KO vs Control conditions.

References

1. Chen S *et al.* (2022) **A genome-wide mutational constraint map quantified from variation in 76,156 human genomes** *bioRxiv*
2. Bernstein A, Chabot B, Dubreuil P, Reith A, Nocka K, Majumder S, Ray P, Besmer P (1990) **The mouse W/c-kit locus** *Ciba Found Symp* **148**:158–66
3. Yarden Y, Kuang WJ, Yang-Feng T, Coussens L, Munemitsu S, Dull TJ, Chen E, Schlessinger J, Francke U, Ullrich A (1987) **Human proto-oncogene c-kit: a new cell surface receptor tyrosine kinase for an unidentified ligand** *EMBO J* **6**:3341–51
4. Lennartsson J, Ronnstrand L (2012) **Stem cell factor receptor/c-Kit: from basic science to clinical implications** *Physiol Rev* **92**:1619–49
5. Keshet E, Lyman SD, Williams DE, Anderson DM, Jenkins NA, Copeland NG, Parada LF (1991) **Embryonic RNA expression patterns of the c-kit receptor and its cognate ligand suggest multiple functional roles in mouse development** *EMBO J* **10**:2425–35
6. Motro B, van der Kooy D, Rossant J, Reith A, Bernstein A (1991) **Contiguous patterns of c-kit and steel expression: analysis of mutations at the W and Sl loci** *Development* **113**:1207–21
7. Hirota S, Ito A, Morii E, Wanaka A, Tohyama M, Kitamura Y, Nomura S (1992) **Localization of mRNA for c-kit receptor and its ligand in the brain of adult rats: an analysis using in situ hybridization histochemistry** *Brain Res Mol Brain Res* **15**:47–54
8. Manova K, Bachvarova RF, Huang EJ, Sanchez S, Pronovost SM, Velazquez E, McGuire B, Besmer P (1992) **c-kit receptor and ligand expression in postnatal development of the mouse cerebellum suggests a function for c-kit in inhibitory interneurons** *J Neurosci* **12**:4663–76
9. Telfer MA, Sugar M, Jaeger EA, Mulcahy J (1971) **Dominant piebald trait (white forelock and leukoderma) with neurological impairment** *Am J Hum Genet* **23**:383–9
10. Finucane B, Scott CI, Kurtz MB (1991) **Concurrence of dominant piebald trait and fragile X syndrome** *Am J Hum Genet* **48**
11. Funderburk SJ, Crandall BF (1974) **Dominant piebald trait in a retarded child with a reciprocal translocation and small intercalary deletion** *Am J Hum Genet* **26**:715–22
12. Lacassie Y, Thurmon TF, Tracy MC, Pelias MZ (1977) **Piebald trait in a retarded child with interstitial deletion of chromosome 4** *Am J Hum Genet* **29**:641–2
13. Kilsby AJ, Cruwys M, Kukendrajah C, Russell-Eggitt I, Raglan E, Rajput K, Lohse P, Brady AF (2013) **Homozygosity for piebaldism with a proven KIT mutation resulting in depigmentation of the skin and hair, deafness, developmental delay and autism spectrum disorder** *Clin Dysmorphol* **22**:64–7
14. Gore BB, Wong KG, Tessier-Lavigne M (2008) **Stem cell factor functions as an outgrowth-promoting factor to enable axon exit from the midline intermediate target** *Neuron* **57**:501–10

15. Su Y, Cui L, Piao C, Li B, Zhao LR (2013) **The effects of hematopoietic growth factors on neurite outgrowth** *PLoS One* **8**
16. Guijarro P, Wang Y, Ying Y, Yao Y, Jieyi X, Yuan X (2013) **In vivo knockdown of cKit impairs neuronal migration and axonal extension in the cerebral cortex** *Dev Neurobiol* **73**:871–87
17. Mashayekhi F, Gholizadeh L (2011) **Administration of anti-c-kit antibody into the cerebrospinal fluid leads to increased cell death in the developing cerebral cortex** *Saudi J Biol Sci* **18**:261–6
18. Aoki H, Hara A, Kunisada T (2017) **Induced haploinsufficiency of Kit receptor tyrosine kinase impairs brain development** *JCI Insight* **2**
19. Kim D, Im JO, Won YJ, Yoon SY, Lee EJ, Lee JH, Hong HN (2003) **Upregulation of c-Kit receptor and stem cell factor in cerebellar inhibitory synapses in response to kainic acid** *J Neurosci Res* **71**:72–8
20. Skarnes WC *et al.* (2011) **A conditional knockout resource for the genome-wide study of mouse gene function** *Nature* **474**:337–42
21. Ohyama T, Groves AK (2004) **Generation of Pax2-Cre mice by modification of a Pax2 bacterial artificial chromosome** *Genesis* **38**:195–9
22. Heintz N (2004) **Gene expression nervous system atlas (GENSAT)** *Nat Neurosci* **7**
23. Ding L, Saunders TL, Enikolopov G, Morrison SJ (2012) **Endothelial and perivascular cells maintain haematopoietic stem cells** *Nature* **481**:457–62
24. Barski JJ, Dethleffsen K, Meyer M (2000) **Cre recombinase expression in cerebellar Purkinje cells** *Genesis* **28**:93–8
25. Fricano-Kugler CJ, Williams MR, Salinaro JR, Li M, Luikart B (2016) **Designing, Packaging, and Delivery of High Titer CRISPR Retro and Lentiviruses via Stereotaxic Injection** *J Vis Exp*
26. Luikart BW, Schnell E, Washburn EK, Bensen AL, Tovar KR, Westbrook GL (2011) **Pten knockdown in vivo increases excitatory drive onto dentate granule cells** *J Neurosci* **31**:4345–54
27. Williams MR, DeSpensa T, Li M, Gulledege AT, Luikart BW (2015) **Hyperactivity of newborn Pten knock-out neurons results from increased excitatory synaptic drive** *J Neurosci* **35**:943–59
28. Martin FH *et al.* (1990) **Primary structure and functional expression of rat and human stem cell factor DNAs** *Cell* **63**:203–11
29. Huang EJ, Nocka KH, Buck J, Besmer P (1992) **Differential expression and processing of two cell associated forms of the kit-ligand: KL-1 and KL-2** *Mol Biol Cell* **3**:349–62
30. Flanagan JG, Chan DC, Leder P (1991) **Transmembrane form of the kit ligand growth factor is determined by alternative splicing and is missing in the Sld mutant** *Cell* **64**:1025–35
31. Langley KE *et al.* (1994) **Properties of variant forms of human stem cell factor recombinantly expressed in Escherichia coli** *Arch Biochem Biophys* **311**:55–61

32. Nitta K, Matsuzaki Y, Konno A, Hirai H (2017) **Minimal Purkinje Cell-Specific PCP2/L7 Promoter Virally** *Mol Ther Methods Clin Dev* **6**:159–170
33. Zaman T, Lee K, Park C, Paydar A, Choi JH, Cheong E, Lee CJ, Shin HS (2011) **Cav2.3 channels are critical for oscillatory burst discharges in the reticular thalamus and absence epilepsy** *Neuron* **70**:95–108
34. Maricich SM, Herrup K (1999) **Pax-2 expression defines a subset of GABAergic interneurons and their precursors in the developing murine cerebellum** *J Neurobiol* **41**:281–94
35. Blake JA, Ziman MR (2014) **Pax genes: regulators of lineage specification and progenitor cell maintenance** *Development* **141**:737–51
36. Pfeffer PL, Payer B, Reim G, di Magliano MP, Busslinger M (2002) **The activation and maintenance of Pax2 expression at the mid-hindbrain boundary is controlled by separate enhancers** *Development* **129**:307–18
37. Lee SB *et al.* (2011) **PAX2 regulates ADAM10 expression and mediates anchorage-independent cell growth of melanoma cells** *PLoS One* **6**
38. Wehrle-Haller B (2003) **The role of Kit-ligand in melanocyte development and epidermal homeostasis** *Pigment Cell Res* **16**:287–96
39. Besmer P, Manova K, Duttlinger R, Huang EJ, Packer A, Gyssler C, Bachvarova RF (1993) **The kit-ligand (steel factor) and its receptor c-kit/W: pleiotropic roles in gametogenesis and melanogenesis** *Dev Suppl* :125–37
40. Leto K, Carletti B, Williams IM, Magrassi L, Rossi F (2006) **Different types of cerebellar GABAergic interneurons originate from a common pool of multipotent progenitor cells** *J Neurosci* **26**:11682–94
41. Weisheit G, Gliem M, Endl E, Pfeffer PL, Busslinger M, Schilling K (2006) **Postnatal development of the murine cerebellar cortex: formation and early dispersal of basket, stellate and Golgi neurons** *Eur J Neurosci* **24**:466–78
42. Amat SB, Rowan MJM, Gaffield MA, Bonnan A, Kikuchi C, Taniguchi H, Christie JM (2017) **Using c-kit to genetically target cerebellar molecular layer interneurons in adult mice** *PLoS One* **12**
43. Zhou J, Brown AM, Lackey EP, Arancillo M, Lin T, Sillitoe RV (2020) **Purkinje cell neurotransmission patterns cerebellar basket cells into zonal modules defined by distinct pinneau sizes** *Elife* **9**
44. Zhang B, Chen LY, Liu X, Maxeiner S, Lee SJ, Gokce O, Sudhof TC (2015) **Neuroligins Sculpt Cerebellar Purkinje-Cell Circuits by Differential Control of Distinct Classes of Synapses** *Neuron* **87**:781–96
45. Liu Z, Jiang M, Liakath-Ali K, Sclip A, Ko J, Zhang RS, Sudhof TC (2022) **Deletion of Calsyntenin-3, an atypical cadherin, suppresses inhibitory synapses but increases excitatory parallel-fiber synapses in cerebellum** *Elife* **11**
46. Chan-Palay V (1971) **The recurrent collaterals of Purkinje cell axons: a correlated study of the rat's cerebellar cortex with electron microscopy and the Golgi method** *Z Anat Entwicklungsgesch* **134**:200–34

47. Larramendi LM, Lemkey-Johnston N (1970) **The distribution of recurrent Purkinje collateral synapses in the mouse cerebellar cortex: an electron microscopic study** *J Comp Neurol* **138**:451–9
48. Orduz D, Llano I (2007) **Recurrent axon collaterals underlie facilitating synapses between cerebellar Purkinje cells** *Proc Natl Acad Sci U S A* **104**:17831–6
49. Witter L, Rudolph S, Pressler RT, Lahlaf SI, Regehr WG (2016) **Purkinje Cell Collaterals Enable Output Signals from the Cerebellar Cortex to Feed Back to Purkinje Cells and Interneurons** *Neuron* **91**:312–9
50. Kreitzer AC, Carter AG, Regehr WG (2002) **Inhibition of interneuron firing extends the spread of endocannabinoid signaling in the cerebellum** *Neuron* **34**:787–96
51. Kreitzer AC, Regehr WG (2001) **Cerebellar depolarization-induced suppression of inhibition is mediated by endogenous cannabinoids** *J Neurosci* **21**
52. Safo PK, Cravatt BF, Regehr WG (2006) **Retrograde endocannabinoid signaling in the cerebellar cortex** *Cerebellum* **5**:134–45
53. Williams MR, Fuchs JR, Green JT, Morielli AD (2012) **Cellular mechanisms and behavioral consequences of Kv1.2 regulation in the rat cerebellum** *J Neurosci* **32**:9228–37
54. Fuchs JR, Robinson GM, Dean AM, Schoenberg HE, Williams MR, Morielli AD, Green JT (2014) **Cerebellar secretin modulates eyeblink classical conditioning** *Learn Mem* **21**:668–75
55. Wu WY, Liu Y, Wu MC, Wang HW, Chu CP, Jin H, Li YZ, Qiu DL (2020) **Corticotrophin-Releasing Factor Modulates the Facial Stimulation-Evoked Molecular Layer Interneuron-Purkinje Cell Synaptic Transmission in vivo in Mice** *Front Cell Neurosci* **14**
56. Zhou H, Lin Z, Voges K, Ju C, Gao Z, Bosman LW, Ruigrok TJ, Hoebeek FE, De Zeeuw CI, Schonewille M (2014) **Cerebellar modules operate at different frequencies** *Elife* **3**
57. Brochu G, Maler L, Hawkes R (1990) **Zebrin II: a polypeptide antigen expressed selectively by Purkinje cells reveals compartments in rat and fish cerebellum** *J Comp Neurol* **291**:538–52
58. Leclerc N, Dore L, Parent A, Hawkes R (1990) **The compartmentalization of the monkey and rat cerebellar cortex: zebrin I and cytochrome oxidase** *Brain Res* **506**:70–8
59. Sarna JR, Marzban H, Watanabe M, Hawkes R (2006) **Complementary stripes of phospholipase Cbeta3 and Cbeta4 expression by Purkinje cell subsets in the mouse cerebellum** *J Comp Neurol* **496**:303–13
60. Marzban H, Chung S, Watanabe M, Hawkes R (2007) **Phospholipase Cbeta4 expression reveals the continuity of cerebellar topography through development** *J Comp Neurol* **502**:857–71
61. Adachi S, Ebi Y, Nishikawa S, Hayashi S, Yamazaki M, Kasugai T, Yamamura T, Nomura S, Kitamura Y (1992) **Necessity of extracellular domain of W (c-kit) receptors for attachment of murine cultured mast cells to fibroblasts** *Blood* **79**:650–6

62. Tabone-Eglinger S, Calderin-Sollet Z, Pinon P, Aebischer N, Wehrle-Haller M, Jacquier MC, Boettiger D, Wehrle-Haller B (2014) **Niche anchorage and signaling through membrane-bound Kit-ligand/c-kit receptor are kinase independent and imatinib insensitive** *FASEB J* **28**:4441–56
63. Ango F, di Cristo G, Higashiyama H, Bennett V, Wu P, Huang ZJ (2004) **Ankyrin-based subcellular gradient of neurofascin, an immunoglobulin family protein, directs GABAergic innervation at purkinje axon initial segment** *Cell* **119**:257–72
64. Buttermore ED, Piochon C, Wallace ML, Philpot BD, Hansel C, Bhat MA (2012) **Pinceau organization in the cerebellum requires distinct functions of neurofascin in Purkinje and basket neurons during postnatal development** *J Neurosci* **32**:4724–42
65. Telley L, Cadilhac C, Cioni JM, Saywell V, Jahannault-Talignani C, Huettl RE, Sarrailh-Faivre C, Dayer A, Huber AB, Ango F (2016) **Dual Function of NRP1 in Axon Guidance and Subcellular Target Recognition in Cerebellum** *Neuron* **91**:1276–1291
66. Cioni JM, Telley L, Saywell V, Cadilhac C, Jourdan C, Huber AB, Huang JZ, Jahannault-Talignani C, Ango F (2013) **SEMA3A signaling controls layer-specific interneuron branching in the cerebellum** *Curr Biol* **23**:850–61
67. Wu WC, Bradley SP, Christie JM, Pugh JR (2022) **Mechanisms and Consequences of Cerebellar Purkinje Cell Disinhibition in a Mouse Model of Duchenne Muscular Dystrophy** *J Neurosci* **42**:2103–2115
68. Wisden W, Murray AJ, McClure C, Wulff P (2009) **Studying Cerebellar Circuits by Remote Control of Selected Neuronal Types with GABA(A) Receptors** *Front Mol Neurosci* **2**
69. Bonnan A, Zhang K, Gaffield MA, Christie JM (2023) **Expression of a Form of Cerebellar Motor Memory Requires Learned Alterations to the Activity of Inhibitory Molecular Layer Interneurons** *J Neurosci* **43**:601–612
70. Gaffield MA, Rowan MJM, Amat SB, Hirai H, Christie JM (2018) **Inhibition gates supralinear Ca(2+) signaling in Purkinje cell dendrites during practiced movements** *Elife* **7**
71. Motro B, Wojtowicz JM, Bernstein A, van der Kooy D (1996) **Steel mutant mice are deficient in hippocampal learning but not long-term potentiation** *Proc Natl Acad Sci U S A* **93**:1808–13
72. Katafuchi T, Li AJ, Hirota S, Kitamura Y, Hori T (2000) **Impairment of spatial learning and hippocampal synaptic potentiation in c-kit mutant rats** *Learn Mem* **7**:383–92
73. Kondo T, Katafuchi T, Hori T (2002) **Stem cell factor modulates paired-pulse facilitation and long-term potentiation in the hippocampal mossy fiber-CA3 pathway in mice** *Brain Res* **946**:179–90

Article and author information

Tariq Zaman

Department of Pediatrics & Human Development, College of Human Medicine, Michigan State University

Daniel Vogt

Department of Pediatrics & Human Development, College of Human Medicine, Michigan State University

ORCID iD: [0000-0003-1876-5936](https://orcid.org/0000-0003-1876-5936)

Jeremy Prokop

Office of Research, Corewell Health

Qusai Abdulkhaliq Alsabia

Department of Pediatrics & Human Development, College of Human Medicine, Michigan State University

Gabriel Simms

Department of Pediatrics & Human Development, College of Human Medicine, Michigan State University

April Stafford

Department of Pediatrics & Human Development, College of Human Medicine, Michigan State University

Bryan W. Luikart

Department of Molecular and Systems Biology, Geisel School of Medicine at Dartmouth College

Michael R. Williams

Department of Pediatrics & Human Development, College of Human Medicine, Michigan State University

For correspondence: will3434@msu.edu

ORCID iD: [0000-0003-3310-7181](https://orcid.org/0000-0003-3310-7181)

Copyright

© 2023, Zaman et al.

This article is distributed under the terms of the [Creative Commons Attribution License](https://creativecommons.org/licenses/by/4.0/), which permits unrestricted use and redistribution provided that the original author and source are credited.

Editors

Reviewing Editor

Jun Ding

Stanford University, Stanford, United States of America

Senior Editor

Lu Chen

Stanford University, Stanford, United States of America

Reviewer #1 (Public Review):

This manuscript from Zaman et al., investigates the role of cKit and Kit ligand in inhibitory synapse function at molecular layer interneuron (MLI) synapses onto cerebellar Purkinje

cells (PC). cKit is a receptor tyrosine kinase expressed in multiple tissues, including select populations of neurons in the CNS. cKit is activated by Kit ligand, a transmembrane protein typically expressed at the membrane of connected cells. A strength of this paper is the use of cell-specific knockouts of cKit and Kit ligand, in MLIs and PCs, respectively. In both cases, the frequency of spontaneous or miniature (in the presence of TTX) IPSCs was reduced. This suggests either a reduction in the number of functional inhibitory release sites or reduced release probability. IPSCs evoked by electrical stimulation in the molecular layer showed no change in paired-pulse ratio, indicating release probability is not changed in the cKit KO, and favoring a reduction in the number of release sites. Changes in IPSC amplitude were more subtle, with some analyses showing a decrease and others not. These data suggest that disruption of the cKit-Kit ligand complex reduces the number of functional synapses with only minor changes in synapse strength.

<https://doi.org/10.7554/eLife.89792.2.sa2>

Reviewer #2 (Public Review):

In their study, Zaman et al. demonstrate that deletion of either the receptor tyrosine kinase Kit from cerebellar interneurons or the kit ligand (KL) from Purkinje cells reduces the inhibition of Purkinje cells. They delete Kit or KL at different developmental time points, illustrating that Kit-KL interactions are not only required for developmental synapse formation but also for synapse maintenance in adult animals. The study is interesting as it highlights a molecular mechanism for the formation of inhibitory synapses onto Purkinje cells.

The tools generated, such as the floxed Kit mouse line and the virus for Kit overexpression, may have broader applications in neuroscience and beyond.

One general weakness is that Kit expression is not limited to molecular layer interneurons but also extends to the Purkinje layer and Golgi interneurons. But this expression does not conflict with the principal conclusions, as Purkinje layer interneurons form few or no synapses onto Purkinje cells.

In summary, the data support the hypothesis that the interaction between Kit and KL between cerebellar Molecular Layer Interneurons and Purkinje Cells plays a crucial role in promoting the formation and maintenance of inhibitory synapses onto PCs. This study provides valuable insights that could inform future investigations on how this mechanism contributes to the dynamic regulation of Purkinje cell inhibition across development and its impact on mouse behavior.

<https://doi.org/10.7554/eLife.89792.2.sa1>

Reviewer #3 (Public Review):

Summary: Bidirectional transsynaptic signaling via cell adhesion molecules and cell surface receptors contributes to the remarkable specificity of synaptic connectivity in the brain. Zaman et al., investigates how the receptor tyrosine kinase Kit and its trans-cellular kit ligand regulate molecular layer interneuron (MLI)- Purkinje cell (PC) connectivity in the cerebellum. Presynaptic Kit is specific for MLIs, and forms a trans-synaptic complex with Kit ligand in postsynaptic PC cells. The authors begin by generating Kit cKOs via an EUCOMM allele to enable cell-type specific Kit deletion. They cross this Kit cKO to the MLI-specific driver Pax2-Cre and conduct validation via Kit IHC and immunoblotting. Using this system to examine the functional consequences of presynaptic MLI Kit deletion onto postsynaptic PC cells, they record spontaneous and miniature synaptic currents from PC cells and find a selective

reduction in IPSC frequency. Deletion of Kit ligand from postsynaptic PC cells also results in reduced IPSC frequency, together supporting that this trans-synaptic complex regulates GABAergic synaptic formation or maturation. The authors then show that sparse Kit ligand overexpression in PCs decreases neighboring uninfected control sIPSCs in a potential competitive manner.

Strengths: Overall, the study addresses an important open question, the data largely supports the authors conclusions, the experiments appear well-performed, and the manuscript is well-written. I just have a few suggestions to help shore up the author's interpretations and improve the study.

Weaknesses:

The strong decrease in sIPSC frequency and amplitude in control uninfected cells in Figure 4 is surprising and puzzling. The competition model proposed is one possibility, and I think the authors need to do additional experiments to help support or refute this model. The authors can conduct similar synaptic staining experiments as in Fig S4 but in their sparse infection paradigm, comparing synapses on infected and uninfected cells. Additional electrophysiological parameters in the sparse injection paradigm, such as mIPSCs or evoked IPSCs, would also help support their conclusions.

The authors should validate KL overexpression and increased cell surface levels using their virus to support their overexpression conclusions.

<https://doi.org/10.7554/eLife.89792.2.sa0>

Author Response

The following is the authors' response to the original reviews.

Reviewer #1 (Recommendations for The Authors):

Major comments:

- 1. The immunolabeling data in Figure S4 shows no change in puncta number but reduced puncta size in Kit KO. sIPSC data show reduced frequency but little change in amplitude. These data would seem contradictory in that one suggests reduced synaptic strength, but not number, and the other suggests reduced synapse number, but not strength. How do the authors reconcile these results?*

Regarding the synaptic puncta, In Kit KO (or KL KO), we have not detected an overt reduction in the average VGAT/Gephyrin/Calbindin positive puncta density or puncta size per animal. With respect to puncta size, only in the Kit KO condition, and only when individual puncta are assessed does this modest (~10%) difference in size become statistically significant. In the revision, we eliminate this figure and focus on the per animal averages.

We interpret that the reduction in sIPSC and mIPSC frequency likely stems from a decreased proportion of functional synapse sites. The number of MLIs, their action potential generation, the density of synaptic puncta, and the ability of direct stimulation to evoke release and equivalent postsynaptic currents, are all similar in Control vs Kit KO. It is therefore feasible that a reduced frequency of postsynaptic inhibitory events is due to a reduced ability of MLI action potentials to invade the axon terminal, and/or an impaired ability for depolarization to drive (e.g. coordinated calcium flux) transmitter release. That is, while the number of MLIs and their synapses appear similar, the reduced mIPSC frequency suggests that there is a reduced proportion of, or probability that, Kit KO synapse sites that function properly.

1. Related to point 1, it would be helpful to see immunolabeling data from Kit ligand KO mice? Do these show the same pattern of reduced puncta size but no change in number?

Although we have not added a figure, we have now added experiments and a corresponding analysis in the manuscript. As we had previously for Kit KO, we now for KL KO conducted IHC for VGAT, Gephyrin, and Calbindin, and we analyzed triple-positive synaptic puncta in the molecular layer of Pcp2 Cre KL KO mice and Control (Pcp2 Cre negative, KL floxed homozygous) mice. We did not find a gross reduction in the average synaptic puncta size or density, or in the PSD-95 pinceau size. From this initial analysis, it appears that the presynaptic hypotrophy is more notable in the receptor than in the ligand knockout. We speculate that this is perhaps because the Kit receptor may have basal activity in the absence of Kit ligand, that Kit may serve a presynaptic scaffolding role that is lost in the receptor (but not the ligand) knockout, or simply that the embryonic timing of the Pax2 Cre vs Pcp2 Cre recombination events is more relevant to pinceaux development, especially as basket cells are born primarily prenatally.

1. The data using KL overexpression in PC (figure 4E,F) are intriguing, but puzzling. The reduction in sIPSC frequency and amplitude in the control PC is much greater than seen in the Kit or KL KO. The interpretation of these data, "Thus, KL-Kit levels may not set the number of MLI:PC release sites, but may instead influence the proportion of synapses that are functional for neurotransmission (Figure 4G)" is not clear and the reasoning here should be explained in more detail, perhaps in the discussion.

We have attempted to clarify this portion of the manuscript by eliminating the cartoon of the proposed model, and by revising and adding to the discussion. Either MLI Kit KO or PC KL KO seems to preserve the absolute number of MLI:PC anatomical synapse sites (IHC) but to reduce the proportion of those synapse that are contributing to neurotransmission (mIPSC). We speculate that sparse PC KL overexpression (OX) may either 1) weaken inhibition to surrounding control PCs by either diminishing KL OX PC to KL Control PC inhibition, and/or 2) act retrogradely through MLI Kit to potentiate MLI:MLI inhibition, reducing the MLI:PC inhibition at neighboring Control PCs.

Minor comments:

1. In the first sentence of the results, should "Figure 1A, B" be "Figure C, D"?

Yes, corrected.

1. The top of page 6 states "the mean mIPSC amplitude was ~10% greater in PC KL KO than in control", this does not appear to be the case in Figure 3E. control and KL KO look very similar here.

In this portion of the text citing the modest 10% increase in mIPSC amplitude, we are referring to the average amplitude of all individual mIPSC events in the PC KL KO condition; in the figure referred to by the reviewer (3E), we are instead referring to the average of all mIPSC event amplitudes per KL KO PC. Because of the dramatic difference in sample size for individual events vs cells, this modest difference rises to statistical, if not biological, significance. We include this individual event analysis only to suggest that, since we in fact saw a slightly higher event amplitude in the KL KO condition, it is unlikely that a reduced amplitude would have been a technical reason that we detected a lower event frequency.

1. Figure 3 D, duration, y-axis should be labelled "ms"

Event duration is no longer graphed or referenced. This has been replaced with total inhibitory charge.

Reviewer #2 (Recommendations For The Authors):

Methods:

- *Pax2-Cre line: embryonal Cre lines sometimes suffer from germline recombination. Was this evaluated, and if yes, how?*

The global loss of Kit signaling is incompatible with life, as seen from perinatal lethality in other Kit Ligand or Kit mutant mouse lines or other conditional approaches. Furthermore, a loss of Kit signaling in germ cells impedes fertility. Thus, while not explicitly ruled out, since conditional Pax2 Cre mediated Kit KO animals were born, survived, and produced offspring in normal ratios, we do not suspect that germline recombination was a major issue in this specific study.

- *Include rationale for using different virus types in different studies (AAV vs. Lenti).*

This rationale is now included and reflects the intention to achieve infection sparsity in the smaller and less dense tissue of perinatal mouse brains.

- *How, if at all, was blinding performed for histological and electrophysiological experiments?*

It was not possible for electrophysiology to be conducted blinded for the Kit KO experiments, owing to the subjects' hypopigmentation. However, whenever feasible, resultant microscopy images or electrophysiological data sets were analyzed by Transnetyx Animal ID, and the genotypes unmasked after analysis.

- *Provide justification for limiting electrophysiology recordings to lobule IV/V and why MLIs in the middle third of the molecular layer were prioritized when inhibition of PCs is dominated by large IPSCs from basket cells. Why were 2 different internals used for recording IPSCs and EPSCs in PCs and MLIs? While that choice is justified for action potential recordings, it provides poor voltage control in PC voltage clamp. Both IPSCs and EPSCs could have been isolated pharmacologically using a CsCl internal.*

The rationale for regional focus has been added to the text. For MLI action potential recordings, we opted to sample the middle third of the molecular layer so that we would not be completely biased to either classic distal stellate vs proximal basket subtypes. It is our hope, in future optogenetic interrogations, to simultaneously record the dynamics of all MLI subtypes in a more unbiased way. With respect to internal solutions, we initially utilized a cesium chloride internal to maximize our ability to resolve differences in GABAA mediated currents, which was the hypothesis-driven focus of our study. While we agree that utilizing a single internal and changing the voltage clamp to arrive at per-cell analysis of Excitatory/Inhibitory input would have been most informative, our decision to utilize pharmacological methods was driven by our experience that achieving adequate voltage clamp across large Purkinje cells was often problematic, particularly in adult animals.

Introduction:

In the introduction, the authors state that inactivating Kit contributes to neurological dysfunction - their examples highlight neurological, psychiatric, and neurodevelopmental conditions.

The language has been changed.

General:

Using violin plots illustrates the data distribution better than bar graphs/SEM.

We have included violin plots throughout, and we have changed p values to numeric values, both in the interest of presenting the totality of the data more clearly.

Synapses 'onto' PCs sounds more common than 'upon' PCs.

We have changed the wording throughout.

Figure 1:

1F - there seems to be an antero-posterior gradient of Kit expression.

Though not explicitly pursued in the manuscript, it is possible that such a gradient may reflect differences in the timing of the genesis and maturation of the cerebellum along the AP axis. Regional variability is however now briefly addressed as a motivator for focused studies within lobules IV/V.

E doesn't show male/female ratios but only hypopigmentation.

This language has been corrected.

Figure 2 and associated supplementary figures:

2A/B: The frequency of sIPSCs is very high in PCs, making the detection of single events challenging. How was this accomplished? Please add strategy to the methods.

We have added methodological detail for electrophysiology analysis.

How were multi-peak events detected and analyzed? 'Duration' is not specified - do the authors refer to kinetics? If so, report rise and decay. It is likely impossible to show individual aligned sIPSCs with averages superimposed, given that sIPSCs strongly overlap. Alternatively, since no clear baseline can be determined in between events, and therefore frequency, amplitude, and kinetics quantification is near-impossible, consider plotting inhibitory charge.

Given the heterogeneity of events, we now do not refer to individual event kinetics. As suggested, we have now included an analysis of the total inhibitory charge transferred by all events during the recording epoch.

S2: Specify how density, distribution, and ML thickness were determined in methods. How many animals/cells/lobules?

For consistency with viral injections and electrophysiology, the immunohistochemical analysis was restricted to lobule IV/V. This is clearer in the revision and detail is added in the methods.

S3:

S3B: the labels of Capacitance and Input resistance are switched.

This has been corrected.

How were these parameters determined? Add to methods.

Added

In the previous figure the authors refer to 'frequency', in this figure to 'rate' - make consistent

This has been corrected.

D: example does not seem representative. Add amplitude of current pulse underneath traces.

We added new traces from nearer the group means and we now include the current trace.

F/G example traces (aligned individual events + average) are necessary.

We added example traces near the relevant group means for each condition.

Statement based on evoked IPCSs that 'synapses function normally' is a bit sweeping and can only be fully justified with paired recordings. Closer to the data would be the release probability of individual synapses is similar between control and Kit KO.

Paired recordings in both Kit Ligand and Kit receptor conditional knockout conditions is indeed an informative aim of future studies should support permit. For now, we have clarified the language to be more in line with the reviewer's welcome suggestion.

S4:

Histological strategy cannot unambiguously distinguish MLI-PC and PC-PC synapses. Consider adding this confound to the text.

We have added this confound to the discussion.

The observation that the pinceau is decreased in size could have important implications for ephaptic coupling of MLI and PC and could be mentioned.

We agree and have added this notion to the discussion.

Y-label is missing in B.

Corrected.

Figure 3 and associated supplementary figures:

| *In the text, change PC-Cre to L7-Cre or Pcp2-Cre.*

Changed

| *How do the authors explain a reduction in frequency, amplitude, and duration of sIPSCs in the KL KO but not in the Kit KO? Add to the discussion*

We now address this apparent discordance in the discussion. Pax2 Cre mediates recombination weeks ahead of Pcp2 Cre. We therefore suspect that postnatal PC KL KO may be more phenotypic than embryonic MLI Kit KO because there is less time for developmental compensation. A future evaluation of the impact of postnatal Kit KO would be informative to this end.

| *As in Figure 2, plotting the charge might be more accurate.*

We now plot total charge transfer.

| *Are the intrinsic properties in KL KO PCs altered? (Spontaneous firing, capacitance, input resistance).*

We have added to the text that we found no difference in capacitance or input resistance between Purkinje cells from KL floxed homozygous Control animals versus those from KL floxed homozygous, PCP2 Cre positive KL KO animals. We plan to characterize both basal and MLI modulated PC firing in a future manuscript, especially since Pcp2 Cre mediated KL KO seems more phenotypic than Pax2 Cre mediated Kit KO, we agree that this seems a better testbed for investigating differences in both the basal, and the MLI-mediated modulations in, PC firing.

| *3D-F - Example traces would be desirable (see above, analogous to Fig. 2).*

More example traces have been added.

| *Figure 4: 'In vivo mixtures' sounds unusual. Consider revision (e.g., 'to sparsely delete KL').*

Changed

| *The observation that control PC sIPSC frequency is lower in KL OX PCs than in sham is interesting. This observation would be consistent with overall inhibitory synapse density being preserved. This could be evaluated with immunohistochemistry. For how far away from the injection area does this observation hold true?*

Because we have now analyzed and failed to find an overt (per animal average) change in synaptic puncta size or density in the whole animal Control vs PCP2 Cre mediated KL KO conditions, we do not have confidence that it is feasible to pursue this IHC strategy in the sparse viral-mediated KL KO or OX conditions. To the reviewer's valid point however, we intend to probe the spatial extent/specificity of the sparse phenomenon when we are resourced to complement the KL/Kit manipulations with transgenic methods for evaluating MLI-PC synapses specifically, potentially by GRASP or related methods that would not be confounded by PC-PC synapses. Transgenic MLI access would also facilitate determining the spatial extent to which opto-genetically activated MLIs evoke equivalent responses in Control vs KL manipulated PCs.

| *Y-legend in D clipped.*

Corrected

| *Existing literature suggests that MLI inhibition regulates the regularity of PC firing - this could be tested in Kit and KL mutants.*

For now, based upon transgenic animal availability, we have now included an evaluation of PC firing in the (Pax2 Cre mediated) Kit KO condition. PC average firing frequency, mean ISI, and ISI CV2 were not significantly different across genotypes. A KS test of individual ISI durations for Control vs Kit KO did reveal a difference ($p < 0.0001$). We have added a supplementary figure (S6) with this data. It is possible that in the more phenotypic PC KL KO condition that we may find a difference in these PC spiking patterns of PC firing, however, we are also eager to test in future studies whether postnatal KL or Kit KO impairs the ability of MLI activation to produce pauses or other alterations in PC firing or in PF-PC mediated plasticity.

| **Reviewer #3 (Recommendations For The Authors):**

| *Reference to Figure 1A in the Results section is slightly inaccurate. Kit gene modifications are illustrated in Figures 1A, B. Where Figure 1A shows Kit distribution. Please rephrase. Relatedly, the reference to Figs 1B - D are shifted in the results section, and 1E is skipped.*

We have changed the text.

| *Please show cumulative histograms for frequency too for consistency with amplitude (e.g. Fig 2).*

We have instead, for reasons outlined by other reviewers, documented total charge transfer for both Kit KO and KL KO experiments where sIPSC events were analyzed.

| *Fig S3: include example traces of PPR.*

This is now included.

| *Include quantifications of GABAergic synapse density in Fig S4.*

This is now included.

| *Include inset examples of KO in Fig S4A.*

This is now included.

| *Add average puncta size graphs along Figure S4B. The effect apparent in the histogram of S4B is small and statistics using individual puncta as n values (in the 20,000s) therefore misleading.*

Per animal analysis is now instead included in the figure and text.

| *Figure S4B y axis label blocked.*

Corrected

| *Include quantification referenced in "As PSD95 immunoreactivity faithfully follows multiple markers of pinceaux size 40, we quantified PSD95 immunoreactive pinceau area and determined that pinceaux area was decreased by ~50% in Kit KO (n 26 Control vs 43 Kit KO, $p < 0.0001$, two-tailed t-test)."*

We added a graph of per animal averages, instead of in text individual pinceau areas.

| *Include antibody dilutions in the methods.*

Added.

| *It's unclear from the text where the Mirow lab code comes from.*

Detail has now been added in text.

| *Typo in methods "The Kit tm1c allele was bred..."*

Corrected

| *Typo in Figure S4 legend "POSD-95 immuno-reactivity".*

Corrected